ABSTRACT

LIU, WENBO. Enhanced Comfort and Faster Drying Textile Finish. (Under the direction of Dr. Stephen Michielsen and Dr. Jon P. Rust).

In recent years, there has been great progress in the development of active sports fabrics which aims to perform high functions and to achieve more comfort. For moisture management, the major concerns are moisture from sweating and whether the fabrics stick to the skin or not. These can be modified by changing the cross sections of the fibers and by using special finishing chemicals. The purpose of such fabric is to keep the body dry by keeping moisture away from the body surface in vapor and/or liquid form, and thus gives us a better comfort feeling.

The wetting and wicking behaviors for 3 kinds of fabrics composed of different cross section fibers provided by Eastman have been studied. The fabrics were divided by the type of yarns, which are made of hydrophilic yarns or polyester yarns, and the blend of those two kinds of yarns. The hydrophilic yarn has a special morphology because the cross section of fibers provide more surface area compared with polyester yarns, which led to larger wicking area. Based on these properties, the wetting and wicking area and drying time have been measured for those 3 fabrics, and also the moisture management tests (MMT) have been applied to them.

In order to achieve better comfort feeling on sports fabrics, innovative textile science and technology should be used in the manufacture of sports and leisurewear fabrics. Chemical surface treatment could be applied to large surface area directly during fabric finishing. The chemical grafting methods have high efficiency and low cost when using chemicals that can react with the active groups on fiber surfaces, such as carboxyl groups and hydroxyl groups. Highly functional polymer poly(acrylic acid), PAA, was used for the first step of treatment, which provide plenty of react groups on the fabric surface. Then long chain alcohols were reacted with PAA in order to achieve hydrophobic properties for the inner parts of yarns. This leads to lower water pick up so that the fabric could dry faster and also has a dry look. The comfort of a fabric during exercise can be influenced by the changeable heat and humidity, so dynamic heat and moisture management is needed for better products. We use PNIPAM (poly(N-isopropylacrylamide)) for further treatment, a significant temperature sensitive polymer, which exhibits different solubility under different temperature.

In this study, the principle of wetting and wicking properties of the fabric based on the thermodynamic theories has been determined. Meanwhile, we have modified a knit fabric with dynamic moisture management properties and optimized the process for further commercial use.

© Copyright 2018 Wenbo Liu

All Rights Reserved

Enhanced Comfort and Faster Drying Textile Finish.

by
Wenbo Liu

A dissertation submitted to the Graduate Faculty of
North Carolina State University
in partial fulfillment of the
requirements for the degree of
Doctor of Philosophy

Fiber and Polymer Science

Raleigh, North Carolina

2018

APPROVED BY:

Dr. Stephen Michielsen Committee Co-chair	Dr. Jon Rust Committee Co-chair
Dr. Emiel DenHartog	Dr. Peter Hauser

Dr. Joel Pawlak

DEDICATION

To my families and my advisors.

BIOGRAPHY

The author was born in Jining, Shandong province, China. She received her Bachelor of Engineering in Textile Engineering (High Technology Textile) from Donghua University in May 2014. In May, 2015, she received the Master of Science degree in Textile Engineering from College of Textiles at North Carolina State University. In August 2014, she started her Doctor of Philosophy degree in Fiber and Polymer Science from College of Textiles at North Carolina State University.

ACKNOWLEDGMENTS

I would like to express my sincere gratitude to my advisor Prof. Stephen Michielsen for the continuous support of my Ph.D. study and related research, for his patience, motivation, and immense knowledge. His guidance helped me in all the time of research and writing of this dissertation, encouraged me and supported me through my graduate years. I could not have imagined having a better advisor and mentor for my Ph.D. study.

I want to express my special appreciation to Prof. Jon P. Rust, who had been my co-chair for the second and third years of my Ph.D. study. He offered me the best opportunity for my research project and encouraged me all the time. Every time the handshake was full of warmth and trust.

Besides my advisors, I would like to thank the rest of my committees: Prof. Emiel DenHartog, for being on my committee and for providing me with useful instructions. Prof. Peter J. Hauser, Prof. Joel Pawlak, for their help of professional knowledge and encouragement. I would like to thank Jeff Kraus for his help through my lab experiments. In addition, a thank you to Nguyen Vu and Yuya Tanaka, Jingyao Li, Guoqing Li, and Xiaohang Sun who assisted and taught me a lot for my research experiments.

Last but not the least, I wish to express my deepest love and gratitude to my beloved family for their support and understanding all the time.

TABLE OF CONTENTS

LIST OF TABLES

LIST OF FIGURES

1. INTRODUCTON

In recent years, there has been great progress in the development of active sports fabric which aims to perform high functions and to achieve more comfort. The sophisticated technologies are used in technical textiles to produce sportswear, which provide properties such as light weight, ultra-breathable with fast drying and high heat and moisture management abilities.[1] People are paying more attention to sports activities that accelerate the demand for more comfort and specific functions. As the market of sportswear continues to expand, many researchers and industries are developing the functional active fabrics. Properties that are required for sports fabric are:[2]

(1) Sports textile must be comfortable, easy to wear, and easy handling.

(2) Sports textiles fabrics have a very high electrical conductivity, so they can permit the dissipation of electrical charge.

(3) They should be light as possible.

(4) Filament fabrics are made highly effective in moisture management and thus they can wick the moisture, i.e. sweat away from the body and keep the body dry.

(5) Sports textiles should have good perspiration fastness.

(6) This sports fabric should also have the special property of heat conductivity to make it possible for the user to feel cooler in summer and warmer in winter.

(7) Maintain a normal level of bacteria on the skin offering a high level of comfort and personal hygiene, especially during athletic activities.

(8) Sports textile fabrics remove UVA and UVB rays that are dangerous to the skin, and guarantees an improved level of defense compared to the majority of natural and man-made fibers.

(9) It also provides superior strength and durability.

In order to achieve these functions on sports fabrics, innovative textile science and technology should be used in the manufacturing of sports and leisurewear fabrics, the factors for developing active sportswear fabrics are: polymer science, fiber science, production techniques, and surface modification of yarns and fabrics.[3]

The base fiber properties are the main factors of the behavior of the fabric. The shape of cross-section of natural fibers or synthetic fibers is critical to characterize fiber properties such as mechanical properties, wetting behavior, reflectance of light, and their packing into a yarn. The wetting behavior is affected by the cross-sectional shapes, which include circular, lobed cross-sections such as a dog-bone, and triangular cross-section shapes, which affect hydrophobicity by reducing the liquid-solid contact areas or hydrophilicity by increasing the liquid wetting areas.[4, 5]

Also, the presence of chemical treatments will modify the properties of fabric as well.[4] Newly developed polymers can have specific properties which are used on sports fabrics, such as “shape memory polymer”, that can remember and retain its shape or return to a previous form. The modification of fabric structure in the finishing step can provide various features like durable water repellency or superior breathability. Layered fabrics also became common for active sportswear. The performance of layered fabric in thermophysiological regulation is better than single layer textile structure.[5]

Considering the trend that the sportswear manufacturing textile industries have already moved their eyes on textile science and technology, various active sports fabric products have come out in order to meet the consumer demand. Based on the existing sports

fabric, we proposed to add dynamic moisture management properties to the fabric for better comfort during exercise.

This project will achieve the following objectives:

(1) Understand the principle of wetting and wicking properties of the fabric based on the thermodynamic theories.

(2) Study the wetting and wicking behavior of fabrics composed by different type of fibers with various cross section shapes.

(3) Modify the knit fabric with dynamic moisture management properties and optimize the process for further commercial use.

2. LITERATURE REVIEW

2.1 Wetting and wicking

2.1.1 Basic surface characteristics

2.1.1.1 Surface tension

The surface tension is the first and most basic aspect of the interface behavior. There are many natural phenomena which are caused by the surface tension, like maintaining the shape of a water droplet or a soap bubble. As the liquid molecules experience an unbalanced force of attraction at the surface, it always shows an elastic tendency of the liquid in order to keep those surface molecules under a balanced condition. At liquid-air interfaces, surface tension results from the greater attraction of water molecules to each other than to the molecules in the air. For the liquid-solid surface, since it is difficult to measure the surface tension, the surface energy should be used, which is an equivalent way to describe the properties.

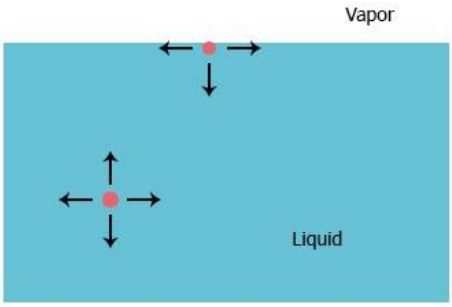

Figure 2-1: Surface tension at the liquid-vapor interface

Figure 2-1 shows the attraction force of the liquid molecules at the interface of the vapor and liquid. In the liquid, the molecules are under a balanced attraction force from all directions. At the interface, there is a lack of the force in the direction perpendicular to the

surface, which leads to the unbalanced condition. We could also view the surface tension as a term of energy, as in the vapor-liquid interface, the molecules at the boundary have a higher energy compared with the ones in the liquid, and the excess energy of the interface can be explained by the thermodynamic theory:[6]

$$\gamma_{LV} = \frac{dG}{dA}\Big|_{V,N,T} \qquad (2.1)$$

This equation shows the surface energy needed when forming an interface. Where γ_{LV} is the surface tension, usually expressed in *N/m* or J/m^2, G is Gibbs free energy of the surface and A is the surface area. The liquid volume is V and number of molecules is N at temperature T.

The interface force, which is dominated by London dispersion forces, hydrogen bonds, and permanent dipoles, is determined by the properties of two media, the contact area and also the environmental factors like temperature and humidity.[7,8]

2.1.1.2 Laplace pressure

As this dissertation focuses on the wetting process of the liquid along fibers, and then spreading along the fabric surface, the capillarity should be considered, which describes the phenomenon for the liquid flow in narrow spaces without external forces. Here, the Laplace pressure as introduced by Young and Laplace is defined as the pressure difference between the inside and the outside of a curved surface of the liquid like a droplet, caused by surface tension.[7] The Laplace pressure is related to the shape of the droplet, and it is critical when we study the behavior of the liquid motion along the surface of the fibers.

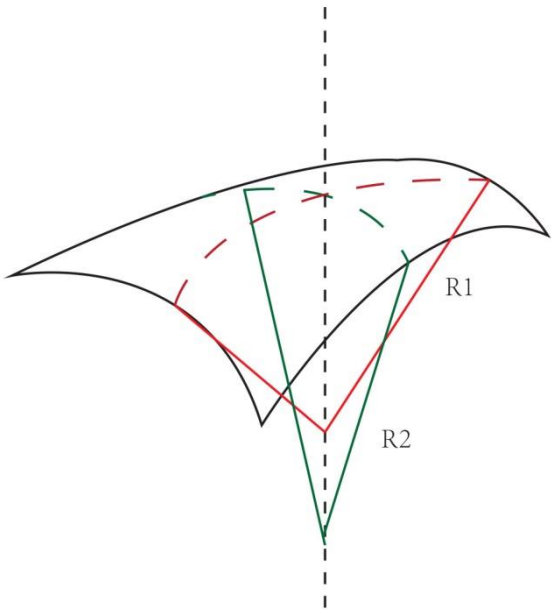

Figure 2-2: Principle radii of a surface

Figure 2-2 shows the shape of a curved surface, where R_1 and R_2 are the two principle radii of the liquid surface. The pressure difference is:

$$\Delta P \equiv P_{inside} - P_{outside} = \gamma_{LV}\left(\frac{1}{R_1} + \frac{1}{R_2}\right) \qquad (2.2)$$

Where P_{inside} is the pressure inside the drop and $P_{outside}$ is the pressure outside the drop. And γ_{LV} refers to the interfacial energy between liquid and vapor. This equation is only valid under equilibrium condition. For each point of the curved surface, the principle radii R_1 and R_2 refer to the maximum and minimum radii at that point. For a drop under equilibrium condition, the Laplace pressure should be the same throughout the entire surface in order to maintain a uniform shape. The simplest model for Laplace pressure is the spherical cap model[8] in which $R_1=R_2$, and the pressure difference becomes:

$$\Delta P = \frac{2\gamma}{R} \qquad (2.3)$$

As we can derive from the Laplace equation, with smaller droplet radii, it should have larger ΔP compared with the big droplet. J. A. Diez[9] worked on the principle of spreading driven by Laplace pressure. He introduced a spreading parameter S, which is firstly proposed as the Young-Dupré equation[10]:

$$S=\gamma_{SG}-\gamma_{SL}-\gamma_{LG} \quad (2.4)$$

The Laplace pressure is found to be the dominate force of droplet spreading on a smooth rigid horizontal surface with a spreading parameter S>0, which indicates the surface is completely wet.

2.1.1.3 Contact angle

For a liquid-solid interface, the contact angle is one of the common ways to describe the wettability of this surface. For the wetting process, which is the ability for liquid to spread on the solid substrate, the contact angle is a direct factor to determine if the liquid is easy to spread on the surface or not. The contact angle measurement is also the first step to determine whether the surface tends to be hydrophobic or not. In the aspect of the thermodynamics theory, Thomas Young proposed the famous Young's equation, which describes the thermodynamic equilibrium condition between three phases: the vapor phase, the solid phase and the liquid phase.[7] This figure shows the equilibrium condition of Young's equaition:

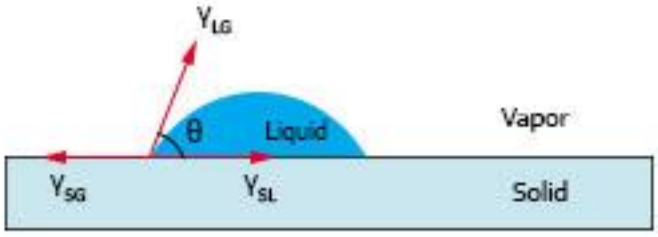

Figure 2-3: Liquid drop on a smooth surface[7]

$$\cos\theta = \frac{\gamma_{SG} - \gamma_{SL}}{\gamma_{LG}} \qquad (2.5)$$

Where θc is Young's contact angle, γ_{LG}, γ_{SG} and γ_{SL} refer to the interfacial energies of liquid-gas, solid-gas and solid liquid, respectively. According to this equation, it is an approach to evaluate the surface tension through the contact angle. Figure 2-4 shows the contact angles of a droplet on a solid surface, where hydrophilic, hydrophobic and superhydrophobic have been introduced.

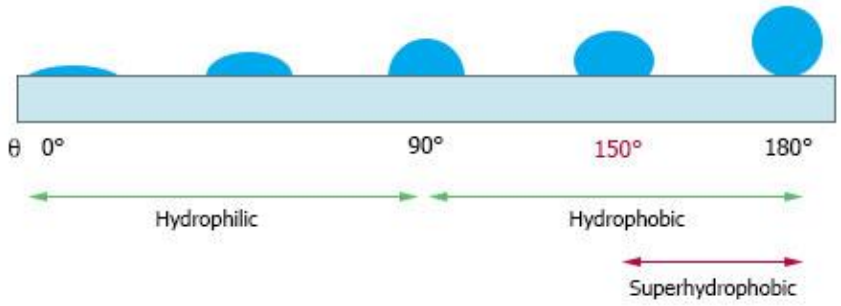

Figure 2-4: Different wettability of the drop on smooth surface[11]

For the liquid contact with the solid surface, if the contact angle is <90∘, the surface is hydrophilic. If the contact angle is >90, the surface is hydrophobic, and when the contact angle is above 150, this surface could be considered as superphydrophobic.

Figure 2-5 shows a droplet rolling off on a tilted solid surface.[11] The roll-off angle refers to the angle at which the droplet completely rolls off from the tilted surface.

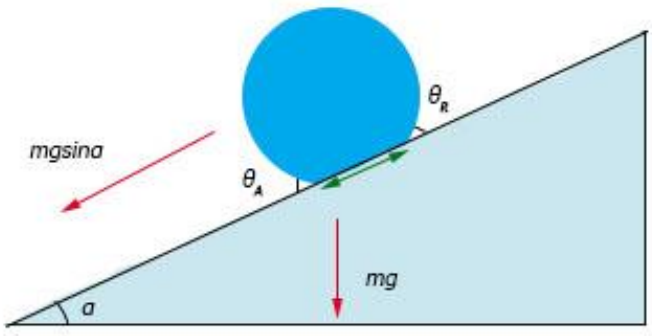

Figure 2-5: Liquid drop rolling of on a tilted solid surface[11]

The roll-off angle is related to the volume of the droplet that gives the gravity effect on the rolling off process. Also the roll-off angle is related to the surface tension of the liquid-solid interface. This equation describes the mechanical equilibrium of a specific point of the process:

$$mgsin\alpha/l = \gamma_{LG}(cos\theta_A - cos\theta_R) \qquad (2.6)$$

Where m is the mass of the droplet, g is the gravitational acceleration, α is the roll-off angle, l is the contact length of the wet area, γ_{LG} γ_{LG} is the liquid-vapor interfacial energy, θ_A is the advancing contact angle and θ_R is the receding contact angle.

Continuing from Young's equation, Athanase Dupre at 1869 worked on the adhesion of two immiscible liquid and gave this equation:[12]

$$W_{ab} = \gamma_a + \gamma_b - \gamma_{ab} \qquad (2.7)$$

Where W_{ab} is the work of adhesion of the two liquid phases, the work of adhesion could be measured by the surface tension of these two phases and the interfacial energy

between these two phases. Then this equation has been expanded as two condensed phases a and b. When we consider a and b to be solid surfaces, substituting Young's equation into the above equation gives:

$$W_{AB}=\gamma_L\left(1+\cos\theta\right) \qquad (2.8)$$

This work has been given by Adam and Jessop[12] and then rewritten in this final form as for thermodynamic validity by Bangham and Razouk.[12] Where *A* is a solid phase, and *B* is a liquid drop contacting with surface *A*, and θ is the contact angle between *A* and *B*. The adhesion work W_{AB} could also be described as the work required to separate the drop leaving a clean solid surface.

In order to determine $\gamma_{SL,}$ Fowkes[13] gave this equation to describe the surface tension between solid and liquid only under the dispersion interaction.

$$\gamma_{SL}=(\sqrt{\gamma_s}-\sqrt{\gamma_l})^2 \qquad (2.9)$$

So the thermodynamic work can be derived as:

$$W_{SL}=2\sqrt{\gamma_s\gamma_l} \qquad (2.10)$$

Besides these equations above, there is extensive work on the derivation, which applies a good way for us to measure the interfacial energy.

2.1.2 Wetting of rough surfaces

Young's equation and Laplace pressure could be used to describe the wetting behavior of a droplet on the smooth surface. But most of the conditions in nature are rough surfaces, especially for the wetting behavior of fabric surface in the subject of interest to this project.

For liquid contact with a rough surface, the contact angle is no longer the same as introduced from Young's equation. The true and the apparent contact angles are shown in Figure 2-6:[11]

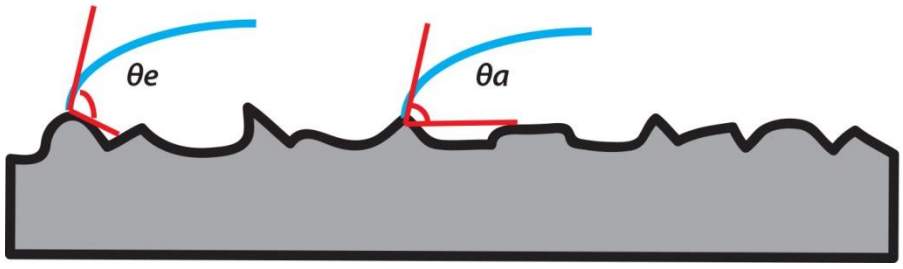

Figure 2-6: Equilibrium contact angle and the apparent contact angle

Where θe is the equilibrium contact angle for a small location on the rough surface. The apparent angle θa is more commonly used to describe the liquid-surface interface. Two models above are Wenzel model and Cassie-Baxter model,[14,15] which describe two different wetting conditions on the rough surface, also could be called complete wetting and composite wetting as the Figure 2-7 shows below:

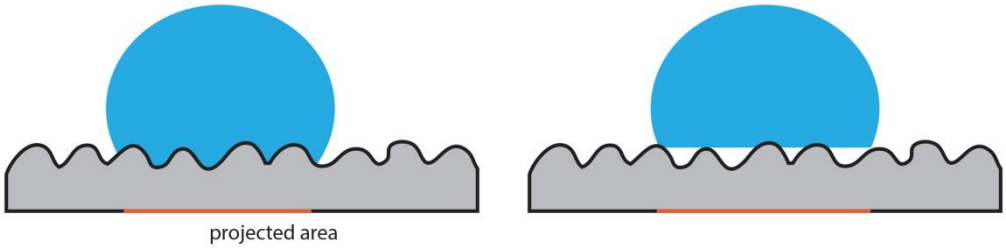

Figure 2-7: Wenzel model (left) and Cassie-Baxter model (right)

Wenzel[15] studied the complete wetting, which is a wetting condition that all the grooves on the rough surface have been completely filled by the liquid. In this study, the contact angle can be described as follows:

$$\cos\theta_{\mathrm{r}}^{W} = r\cos\theta_{e} \qquad (2.11)$$

Where *r* is the roughness factor of the surface, indicating the ratio of the total wet area of a rough surface to the apparent surface area in contact with the liquid. (r>1) So Wenzel apparent contact angle is related with the equilibrium contact angle, Young's contact angle, and the roughness factor of the surface. According to this equation, compared with the flat surface, roughness will contribute to increase the apparent contact angle when $\theta_e > 90°$, which means that the surface will be more hydrophobic.

Another condition shown in the Figure 2-7 is Cassie-Baxter model.[14]

The liquid doses not fill the grooves on the rough surface completely, but to form a composite surface made of liquid, air and solid. They introduced the apparent contact angle θ_{r}^{CB} :

$$\cos\theta_{r}^{CB} = f_1\cos\theta_{e} - f_2 \qquad (2.12)$$

Where f_1 is the true liquid-solid contact area divided by the projected area, f_2 is the liquid-vapor contact area divided by the projected area. Also θ_{e} is the equilibrium contact angle between the liquid and solid. The Cassie-Baxter model could be modified in order to design a rough surface with has high apparent contact angle. The equation represented that the apparent contact angle can be greater than 90° even if the equilibrium contact angle is small, in contrast with Wenzel model. The Cassie-Baxter model indicates that the roughness of a surface plays an important role in improving the liquid repellence property of this surface. Marmur[16] studied the meta-state between Wenzel state with Cassie-Baxter state,

which could describe the transform process of these two models, depending on the local and global minimum Gibbs surface free energy. Here the Cassie-Baxter contact angle could be expressed by *f* and r_f with Wenzel equation:

$$\cos\theta_r^{CB} = r_f f \cos\theta_e + f - 1 \qquad (2.13)$$

Where *f* is the fraction of the projected area that is wet and r_f is the roughness ratio of the wet area. Based on the basic model introduced above, the modification work for the apparent angle on different kinds of fabric structures has been done.[11]

2.1.3 Wicking phenomenon

The basic aspects about wetting have been reviewed above. Despite wetting, another phenomenon, wicking, will happen during the same process for liquid contact with the fibrous material. Wetting and wicking are two important phenomena for the fibrous material, both these processes are related but different from each other. Wetting is the displacement of a solid-air interface with a solid-liquid interface. Wicking is the spontaneous flow of liquid in a porous substrate, driven by capillary forces.[17] Wetting is a prerequisite for wicking, the liquid that does not wet the fibers cannot wick into the fabric. Wicking can only occur when fibers assembled with capillary spaces between them are wetted by a liquid, which is the spontaneous flow of liquid through the capillary which can be visualized as a displacement of a solid-air interface with a solid-liquid interface only in a capillary system. The free energy in this process can be represented by:[7]

$$W_P = \gamma_{SG} - \gamma_{SL} \qquad (2.14)$$

Where *Wp* is the work of capillary penetration, γ_{SG} and γ_{SL} are the interfacial energy of solid-vapor and solid-liquid phase. The capillary system can be seen as a fibrous fabric or

just two parallel fibers. Here the capillary pressure plays an important role in this process. Figure 2-8 shows the capillary pressure of liquid in a narrow cylindrical tube.

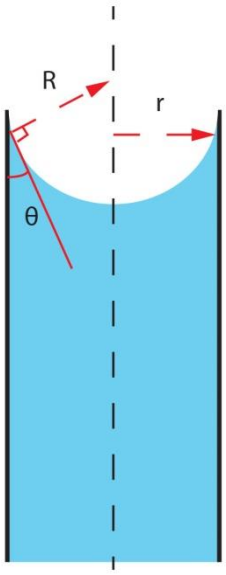

Figure 2-8: Capillary rise in a narrow tube

The pressure difference ΔP is caused by the surface tension, as for the curved interface, the relationship between ΔP and the surface characters could be represented by the Laplace pressure, where the two radii of curvature are equal to each other:[17]

$$\Delta P=2\gamma_{LV}/R \qquad (2.15)$$

When the capillary wall is completely wetted by the liquid, the liquid-vapor interface can be assumed to be a hemisphere and R=r, where r is the capillary radius:

$$\Delta P=2\gamma_{LV}/r \qquad (2.16)$$

When the capillary wall is not completely wet, there is an angle θ between the wall and the liquid.

$$r/R = \cos\theta \qquad (2.17)$$

$$\Delta P=2\gamma_{LV}\cos\theta/r \qquad (2.18)$$

When the capillary pressure reaches the equilibrium state at a height of h, ΔP could also be expressed as:[7]

$$\Delta P=\Delta\rho gh=2\gamma_{LV}/r \quad (2.19)$$

Here we define the capillary constant or the capillary length:

$$\ell_{cap}=r=2\gamma_{LV}/\Delta\rho gh \quad (2.20)$$

This equation combines the liquid density ρ, the height of the liquid in capillary tube, which is easy to measure, with the surface tension of the liquid. In this way, as we could obtain the capillary length in the profile, so the capillary length is also a good way to measure the liquid surface tension. To conclude, the capillary rise is an important phenomenon in wetting and wicking process, the shape of the droplet in a capillary system is dominated by the pressure difference in the curved interface.

2.1.4 Influence by fiber type and yarn structure

The fabric construction consists of the formation of fibers and yarns. For woven fabric, the specific structure results from the interlacements of warp and weft yarns. The knitted structure is formed by a series of yarn loops, weft-knit and warp-knit are two major varieties of knitted fabrics. Fibers can be obtained from plants, animal and silk or synthetic polymers with different cross-sectional shapes, and the types of fibers strongly influence the determination of fabric property.[18,19] The yarns are formed by packing fibers into a yarn, which allows the increase or decrease of the fabric physical or mechanical properties.[20] Therefore, the fiber type, yarn structure and fabric geometry should all be considered for the final properties of the fabric.

The shape of cross-section of natural fibers or synthetic fibers is critical to characterize fiber properties such as mechanical properties, wetting behavior, reflectance of light, and their packing into a yarn. The wetting behavior is effected by the cross-sectional shapes, which include circular, lobed cross-sections such as a dog-bone, and triangular cross-section shapes, which affect hydrophobicity by reducing the liquid-solid contact areas or hydrophilicity by increasing the liquid wetting areas.[21,22] Figure 2-9 shows the different cross-section shapes of both nature fibers and man-made fibers:

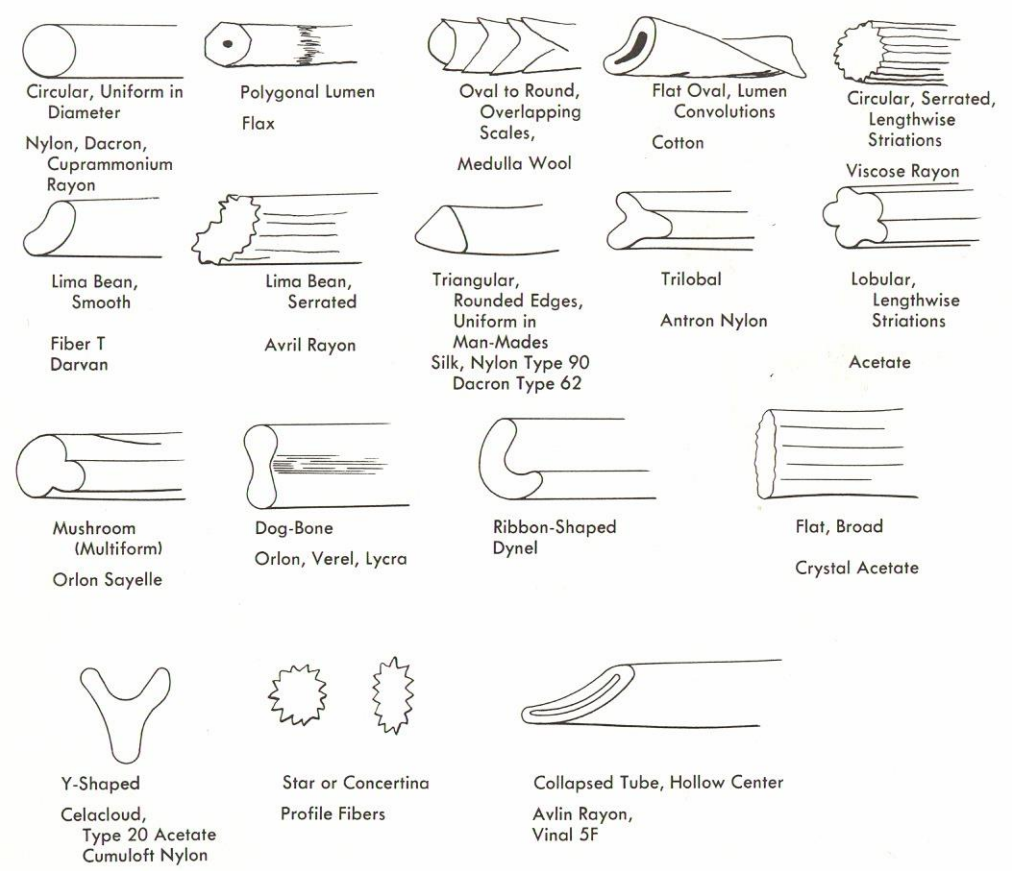

Figure 2-9: Types of cross-section shape of both nature fiber and man-made fiber[23]

The cross-section shape of man-made fibers are manufactured for the required end-use properties and controlled by spinneret design, while natural fibers are genetically developed by their own. Man-made fibers can be homogenous or heterogeneous, depending

on the different type numbers of polymers. A single polymer is used to make homogenous fibers while two or more polymers are used to make heterogeneous fibers which will have different thermal and mechanical properties.

Yarns are classified into filament yarn and spun yarn. The spun yarn is made by twisting relatively short staple yarns together as cohesive thread, which is produced through several processes: blending, cleaning, opening, drawing, and spinning to arrange the fibers for the construction of a yarn. Filament yarn consists of very long continues filament fibers, either twisted together or only grouped together, whose simple structure can be modified by texturing, crimping, or twisting to change or improve the properties of the yarn, such as bulkiness, texture, stretchiness, or strength.

Filament yarns can be classified as monofilament yarn and multifilament yarn as shown in Figure 2-10, a multifilament yarn contains more void spaces compared with monofilament yarn under same linear density. The packing density of the filament yarn is critical to the yarn properties, as tightly packed filaments rarely move while loosely packed filaments easily move under specific pressure.[24]

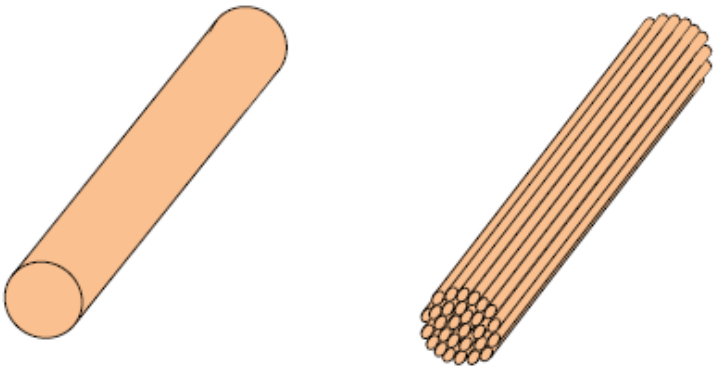

Figure 2-10: Man-made monofilament (left) and multifilament (right)[25]

The cross-section shape of filament fiber is important for the packing density, which will influence the spaces between filaments in a fiber assembly. Compared with circular cross-section shape, other varieties such as multi-lobal or dog-bone shape will pack less closely, which will create larger void spaces within the yarns. With large void spaces, it allows more air permeability, moisture absorption, and quicker drying properties of fabrics. Thus, the space within the yarns is a critical factor for the wetting and wicking properties of fabric.

Also the cross-section shape of filament fiber is related to the porosity of the fabric, which is another important factor for describing the wetting behavior when the fabric has been saturated with water. The porosity of fabric can be calculated from the packing factor of fabric:[26]

$$\phi\% = \frac{\rho_{fabric}}{\rho_{fiber}} \times 100\% \qquad (2.21)$$

Where ρ_{fabric} and ρ_{fiber} correspond to the density of fabric and fiber.

The porosity of fabric is (1- ϕ) * 100%.

2.2 Surface modification

After the introduction of the wetting behavior of the fabric surface, we move to the modification part. The surface of the textile material is indeed the interface or reaction region between the textile and the environment in which the material is used. Wetting, friction, adhesion, biocompatibility and adsorption all begin at the surface.[18] The surface will contact with our skin directly, which we can make a judgement of whether it is a good product or not from its comfort. To improve or change the surface properties for sportswear fabric, there are numerous ways to do the modification. Coating, plasma treatment and surface grafting are three main methods for surface modification. Coating can improve the

surface properties by applying a covering on the object, but they often come off when there is any bending, heat change, abrasion, or other forces applied to it.[19] Plasma treatment is a clean, dry, and environmentally friendly technology but requires very high cost in industrial production. It is used to create active sites on the surface for further functionalization.[18] Surface grafting of textiles is a relatively recent technology that allows several ways to alter the surface of textile materials. Some modifications are highly efficient and low cost using chemicals that can react with the active groups on fiber surfaces, such as carboxyl groups and hydroxyl groups. However, the active groups in fibers are limited, and then initial modification is needed to provide or graft the functional groups on the surface so that further treatment could be continued. Furthermore, in recent years, new technologies for surface modifications have received attention such as high energy beam processes, vapor deposition and nanoparticle coatings. For our research, we focus on the surface grafting on the polymeric fabric which has lower cost and is easier to operate.

2.2.1 Introduction of surface grafting

Grafting is an economical surface treatment that can be used to impart many different properties to a material. As it has been paid more attention, several studies have demonstrated that the properties of polymeric substrates could be altered, or impart new or functional properties on the substrates by surface grafting. There are four primary techniques for surface grafting: (1) chemical graft polymerization; (2) radiation-induced grafting; (3) plasma-induced grafting and (4) light-induced grafting. These four methods are all under the same principle: creating free radical sites within the macromolecules of the substrate. Then, these radical sites are used as initiators for copolymerization reactions with vinyl monomers present in the grafting solution, or the radical sites act as the functional groups that could

have further reaction on it.[18] For these two kinds of grafting, Uyama et al. have illustrated them as direct coupling reaction of existing polymer molecules to the surface and graft polymerization of monomers.[20] Figure 2-11 shows these two methods:

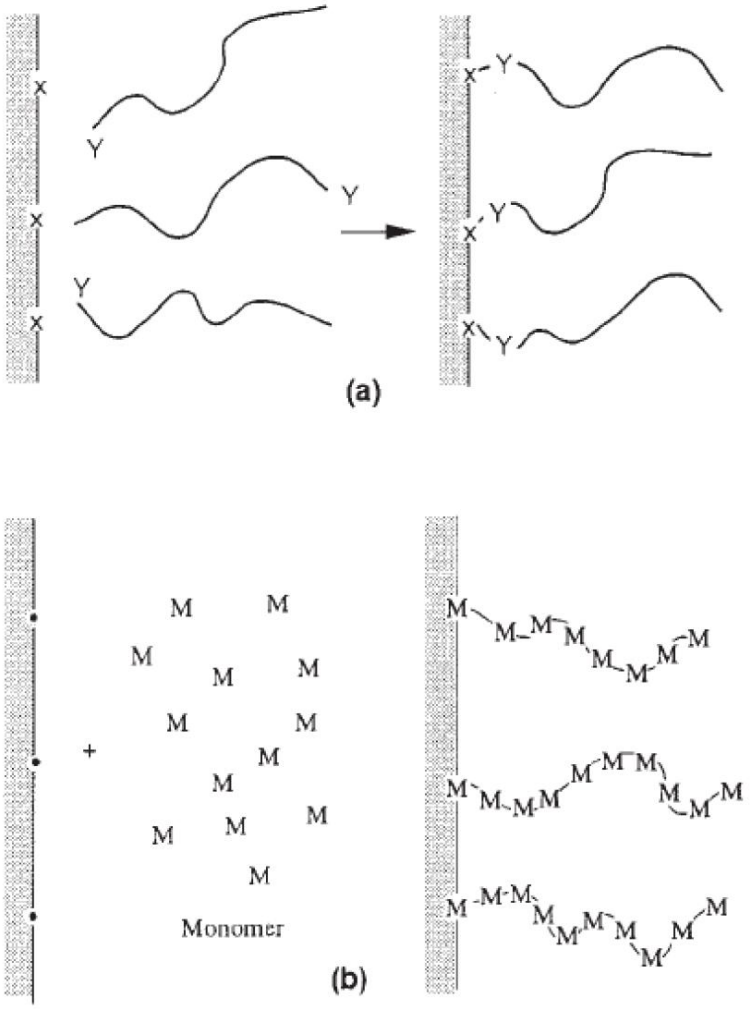

Figure 2-11: (a) Direct coupling of polymers to the surface, (b) Graft polymerization of monomers (Uyama et al., 1998)[20]

We could couple small monomers or long polymer chains onto the surface. We prefer grafting the surface with polymer not monomer because of the density of active sites should be considered. When we graft small molecules onto the surface, a very large number of

grafted sites or high coverage of chemical bonding groups should already exist or be created, but for most daily used polymeric fabrics, the active sites are limited on the surface. So one advantage of using a polymer to modify the surface of polymeric fabric is that fewer grafted sites are needed. A relatively small number of grafted polymer chains can potentially cover the entire surface of the polymer film using only a few graft sites.[21] Based on the two methods introduced above, the polymer grafting can be achieved by grafting the polymer directly on the surface or create a radical first and then use it as the initiator to have further polymerization on the surface. Also, the advantage of polymer grafting includes easy and controllable introduction of polymer chains with a high surface density, precise localization of the chain at the surface, and long stability of the grafted layers.[22] And it is possible to graft several different polymers on the surface which could provide additional functionality. Stamm[22] has concluded these two methods as 'grafting to' and grafting from' the surface. 'Grafting to' is when the polymer chains are grafted to the substrate, the polymer will react with the functional groups on the surface to form chains on the surface directly. This also refers to what we talked about 'direct coupling of polymer to the surface'. The major advantage for 'grafting to' is that it permits the design and construction of the surface polymer under conditions that are best suited for its polymerization and allows it to be characterized fully before use.[21] Also this method is beneficial for continuous manufacture process especially when the time for processing is concerned.

'Grafting from' is when polymerization takes place from the surface. Molecules of a monomer can penetrate through the already grafted polymer layer easily and significant grafted amounts can be reached.[22] This is what we conclude as 'graft polymerization of monomers'. The major disadvantages of this approach are that polymerization times are often

long, and it is difficult to determine the molecular weight of the surface polymer.[20] Also another disadvantage is that the polymerization may not happen only at the surface, it can also react within the surface. As concluded, the 'grafting to' method is better to control the reaction, and easy to modify the surface in the manner we want.

There is another approach to prepare graft copolymers is called 'grafting through'. This method has also been used frequently these days, especially been widely applied in industrial applications.[27] In order to create assemblies of polymers tethered to surfaces, a monomer will be anchored to a substrate and followed by a bulk polymerization reaction to chemically link the growing polymer chains to the surface-bound monomers.[28] For a polymer layer generation through this method, the growth of polymer chains should be initiated in the solution. During propagation, a surface-bound monomer unit can be integrated into the growing chains occasionally, which directly results in a permanent anchoring of the polymer chains. After that, chain growth can proceed and further free or surface- attached units can be added to the growing chain.[27] The graft density and polymer layer thickness can be controlled by adjusting the degree of polymerization of side chains and the backbone.

Preeta and Jan[29] had discussed 'grafting through' on one- dimensional substrates (Figure 2-12), which described the overall reaction scheme for the generation of single layer polymer chain through a "grafting through" process.

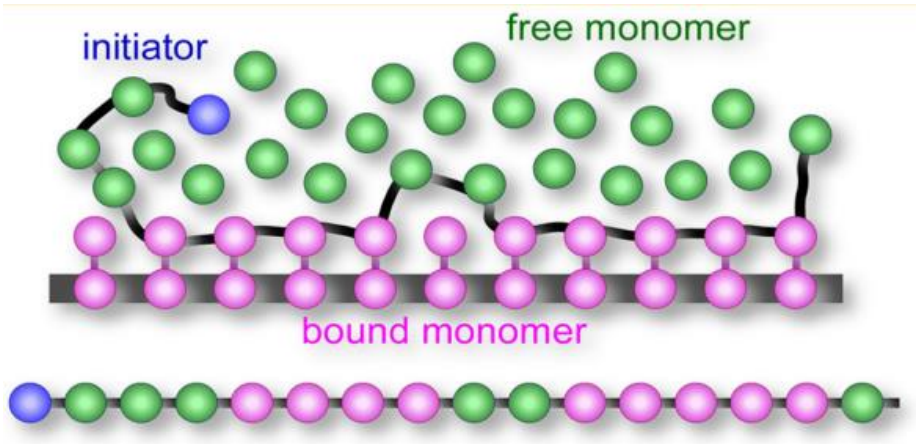

Figure 2-12: 'Grafting through' polymerization[29]

Michael et al.[27] had studied the mechanistic details of 'grafting through' reaction, with a variation of temperature, concentration of initiator or monomer in solution, polymerization time, and the surface-concentration of surface-attached monomer.

Stamm[22] had also investigated the example of polymer chains grafted on the surface: polymer brushes. When high grafting density has been reached, the tethered polymer chains that are connected to the solid substrate by one chain end may be definitely distinguished from other grafted polymer layers. Figure 2-13 shows the representation of polymer brushes:

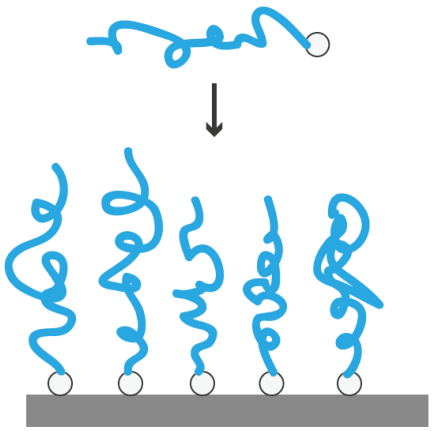

Figure 2-13: Polymer chains forming brushes

Brush-like layers created due to the excluded volume effect, also the properties of brushes are controlled by these parameters: grafting density, chain length, and chemical composition of the chains.[22] In the diluted system, homopolymer brushes would perform in different forms, as figure 2-14 shows.

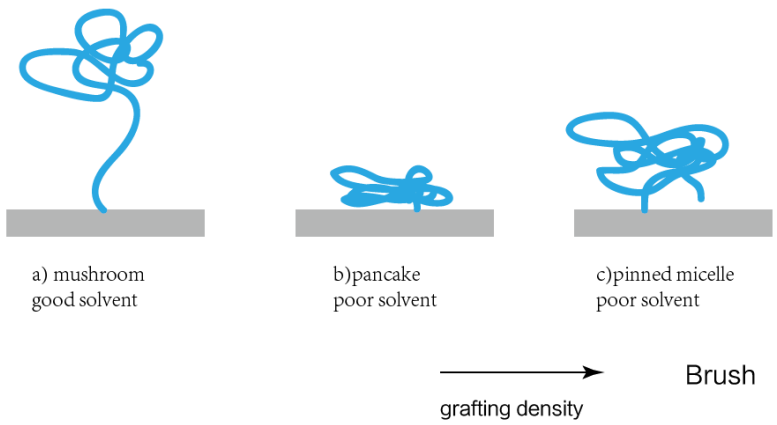

Figure 2-14: a) Diluted good solvent; b) Diluted poor solvent; c) Semi-diluted poor solvent[22]

If the interaction of polymer chains with solvent is stronger than with substrate, the mushroom-like form will be generated, otherwise, the polymer chains will form like pancakes as shown in the figure 2-14. This interaction results either in stretching away from the substrate in good solvent or in the formation of pancake in poor solvent. If the condition is semi-dilute, the polymer chain will interact with neighboring grafts to form like pinned micelle. Despite the homopolymer brushes, there are more kinds of morphology of polymer grafting.

2.2.2 Plasma-induced grafting

In the early 1980s, significant research work of plasma grafting in textile industry has been going on across the world.[30] Various fibrous materials had been applied using low-

pressure treatment and performed improvement in functional properties on the surface since that time. Then after 1998, the low-pressure plasma techniques has been widely used in biomedical applications.[31] This technique is based on the use of activated species, such as ions, radicals, metastable molecules, which are formed by applying a voltage across a space that is filled with gas(O2, N2, etc.) that becomes conductive to create active sites within the structure of the molecules of the substrates, which could be used to initiate copolymerization reactions with different monomers.[18] Despite the high cost, modification of polymer surfaces can be rapidly and cleanly achieved by plasma treatment, with the possibility of the formation of various active species on the surface of polyethylene, polypropylene, etc.[32] Plasma treatments can be complicated with different plasma processing types, but requires higher level of knowledge labor.

2.2.3 Radiation-Induced Grafting

Radiation-induced grafting is a well-established technology which dates back almost 50 years when cellulose was graft-copolymerized with styrene irradiated by γ-Co60 rays in water.[33] Some of the methods for radiation-induced grafting include: simultaneous irradiation and grafting through in-situ formed free radicals, grafting through peroxide groups introduced by pre-irradiation, and grafting initiated by trapped radicals formed by pre-irradiation.[18] Figure 2-15 shows how the radiation grafting works:

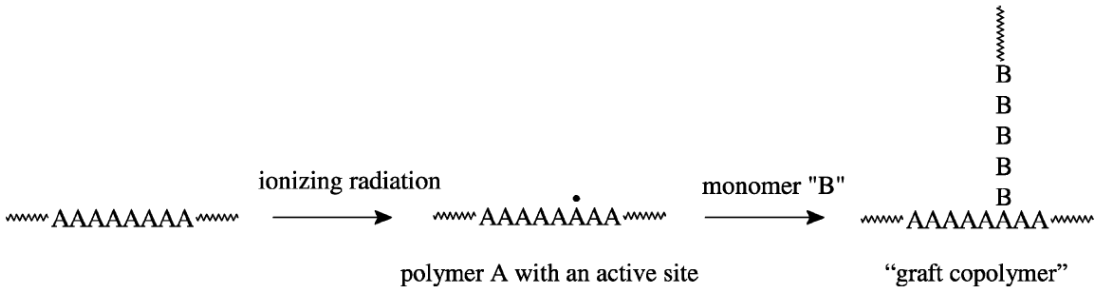

Figure 2-15: The use of ionizing radiation to graft monomer 'B' to polymer 'A' to form a graft copolymer [34]

Here polymer 'A' is exposed to ionizing radiation, the active sites produced randomly along the polymer chain can act as macro-initiators, initiating free radical polymerization of the monomer 'B', in this way polymer B could graft onto polymer A.[34] The advantages for this technology are that this method is capable for many monomer/polymer combinations and chemical initiators are not required.

2.2.4 Light – induced grafting

Light-induced radical polymerization is another excellent option for surface modifications of fibers and fabrics because of its simplicity, safety, and the low energy. As Figure 2-16 shows, the photoinitiator is excited by light to form radical species, and proceeds in the same manner as other radical polymerizations, monomers react with the reactive species to continue the polymerization.[35] Grafting efficiency can be controlled by time, temperature, and concentration of the initiators. [18]

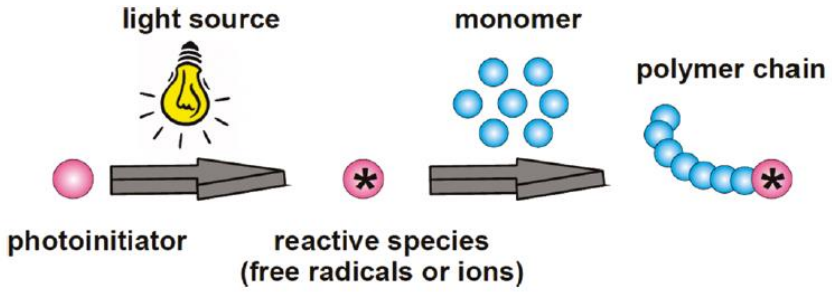

Figure 2-16: General presentation for light-induced polymerization [35]

2.2.5 Chemical grafting

Chemical grafting is a high efficiency and low cost approach which has been applied to several applications. Some modifications are one step using chemicals that can react with functional groups on the fiber surface like carboxyl groups and hydroxyl groups. One can also pre-modify first to create active site for the following polymerization. In our project, we are more focusing on the first approach, directly coupling the polymer onto the surface, because this method tends to be a commercially viable procedure, which could be scaled up later. However, the active sites on fiber surface are limited, it is better to use long chain polymers to do the pretreatment providing high density active sites for the further modification as we have introduced above.

To cover the surface of fabric as much as possible, we choose poly(acrylic acid), PAA, to do the initial modification on the surface to increase the active groups. (Figure 2-17)

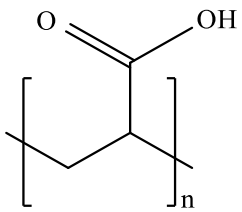

Figure 2-17: Chemical structure of PAA

Poly(acrylic acid) is a high functional polymer that is ideal for grafting. Once it has formed covalent bonds with the fiber surface, it could introduce many carboxylic acid groups for further reactions.

In 1996, Jadwiga[36] investigated the grafting of acrylic acid on PET using benzoyl peroxide, where a radical polymerization happened on the surface. The carboxylic acid groups had successfully grafted on the PET fiber surface, which resulted in a significant increase in their hygroscopicity as well as their swelling in water.[36] This method has also been used for the first step of modifying fibers with antibiotic properties.

Tobiesen and Michielsen discovered that PAA can be grafted on the surface of nylon 6,6 using amide linkages to increase the functional sites, 1-ethyl-3-(3-dimethylaminopropyl) carbodiimide hydrochloride (EDC) was used to activate the amidization.[21] This research also showed that lower amounts of EDC could be used for the same amount of grafting if increased temperatures were also used. As PAA could be obtained in a variety of molecular weights, in this research they found that increase the molecular weight of PAA from 5 kD to 250 kD, the surface coverage on nylon 6,6 by could be raised up to 50 percent.[21] This reaction is very mild, fast, and can be done at room temperature at neutral pH. The grafted nylon 6,6 showed significant increase of functional sites compared with the amide groups it owned originally.

Followed by this technology, Sherill et al.[37] used this to graft antimicrobials to the surface of nylon 6,6. Here, protoporphyrin IX (PPIX) and zinc protoporphyrin IX were grafted to the surface using an ethylene diamine bridge and a poly(acrylic acid) scaffold. The molecular weight of poly(acrylic acid) used was 450 kD. X-ray photoelectron spectroscopy was used to determine that around 57% of the nylon surface was covered by poly(acrylic

acid).[37] And about 6% of the carboxylic acid groups in PAA were converted to PPIX which shows that antimicrobial chemicals could be permanently covalently bonded to the surface of nylon 6,6.

The amount of PAA grafted on the fabric surface can be quantified by a colorimetric method using Toluidine Blue O (TBO), which was based on the number of carboxyl groups grafted onto the fabric. It was estimated based on weight per unit weight or per unit surface area. The TBO molecules combine with carboxyl groups of the PAA in alkaline solution (~pH 10.0) forming an electrostatically stable complex. This complex can be easily detached from the surface usually in acetic acid (~pH 2.0) or many other organic solvents.[38]

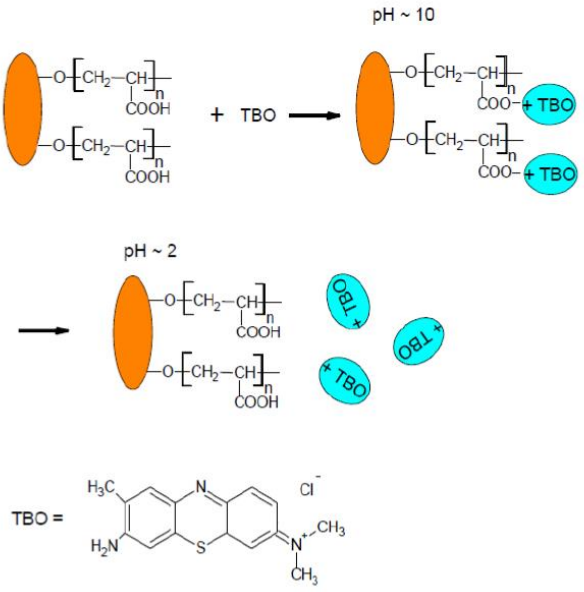

Figure 2-18: Schematic diagram for the quantitative analysis of –COOH groups using Toluidine Blue O[38]

Chemical grafting can be accomplished by a pad-dry and cure procedure which is easy to use in manufacturing. (Figure 2-19) Solutions are made and filled in the bath. Fabrics are continuously sentin to the bath to be covered with solution and then moved through the

padding area. Solutions can be squeezed into the fabric through padding to remove extra solution. Then the fabrics should be sent into an oven where drying and curing happens. This pad-dry-cure procedure is being widely used in dying, and surface modification industry, it can be processed separately and continuously which is advantageous in a manufacturing environment.

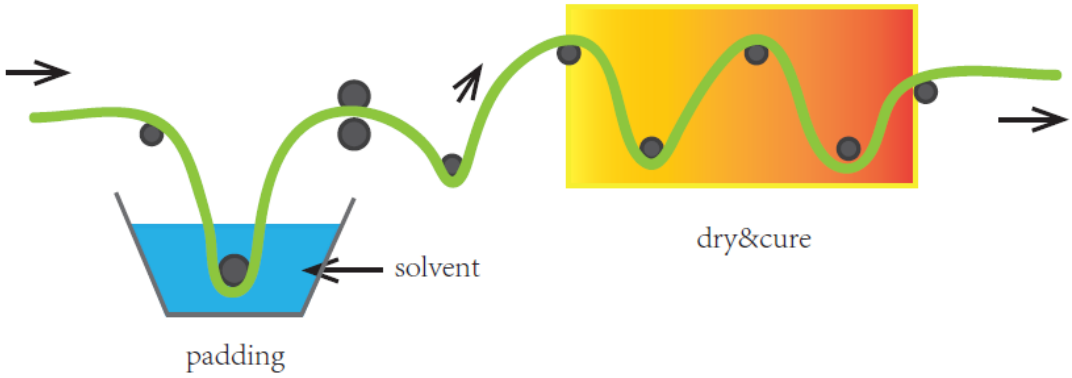

Figure 2-19: Pad-dry-cure procedure

2.3 Dynamic Moisture Management via Hydrogel Treatment

As we have already introduced the wetting behavior and surface modification above, which gives us the way to understand and analyze the basic mechanism of wetting and the procedure for the treatment, now we move to the thermodynamic material treatment on the fabric surface. We propose to graft a kind of thermal responsive polymer on the fabric surface which could have changeable wetting behavior under different temperature so that this fabric will become a 'smart' textile product. Textiles for human clothing are intimate objects with very large surface area for the protection of the body. Therefore, a better thermal exchange with the environment can be developed for the fabric as a smart interface between

human body and the exterior environment. The textile industry nowadays shows a huge interest in environmentally responsive or stimuli-responsive materials that could be incorporated into technical textiles, and the temperature-sensitive polymer is one part of this family.[39] These polymers can be classified on the basis of their solubility, which is widely known by their UCST or LCST properties. The critical solution temperature can be explained by the thermodynamic theory that will be introduced later in detail. One of the best known thermo-sensitive polymers is PNIPAM (poly(N-isopropylacrylamide)), has its lower critical solution temperature (LCST) phenomenon at around 32 ℃ in aqueous solutions.[40] This polymer would be the thermo-sensitive material that we are focusing on the dynamic moisture management of the fabric.

2.3.1 Phase-separation behavior of polymer solution

Polymer solution or polymer blends possess a variety of possible T-φ phase diagram patterns, two of which are depicted in Figure 2-20. The two shown are upper and lower critical temperature phase boundaries. If the polymer solution tends to have phase separation upon cooling, this transition is labeled an upper critical solution temperature (UCST), on the contrary, of the phase separation happens when the temperature goes up, this transition is labeled an lower critical solution temperature (LCST).

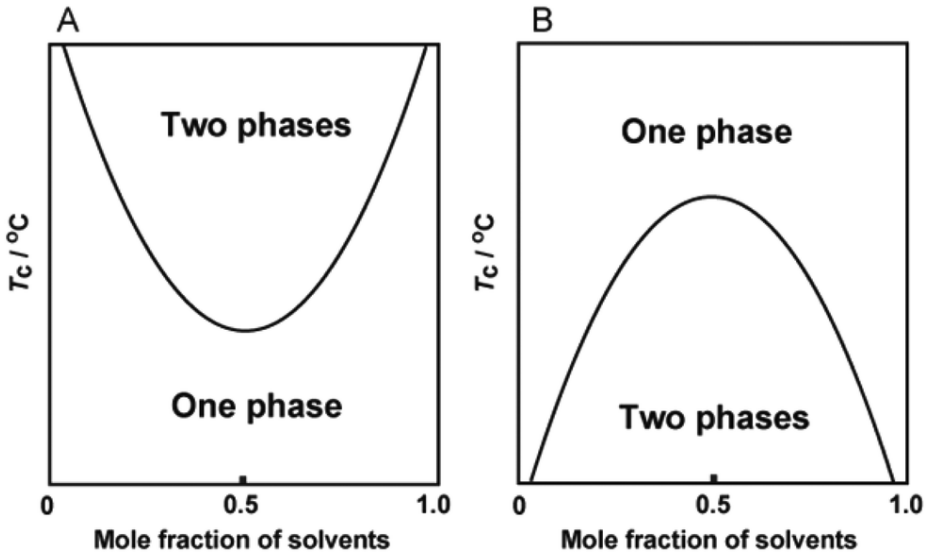

Figure 2-20: Schematic illustration of typical phase diagrams of LCST behavior (A) and UCST behavior (B).[41]

Many texts have explained the thermodynamics of polymer blends and block copolymers, which was first systematically proposed as Flory-Huggins theory.[42,43] The phase behavior of polymer solution can be described, like other mixtures, by the Gibb's free energy of mixing (ΔG_m), which is dependent on both the enthalpy (ΔH_m) and entropy (ΔS_m) changes on mixing, and is negative for favorable processes.[44]

$$\Delta G_m = \Delta H_m - T\Delta S_m < 0 \qquad (2,22)$$

The effect of temperature upon phase separation of solutions of non-crystallizing polymers is usual to deal with molar quantities, here we give the Flory-Huggins equation for the Gibbs free energy of mixing:

$$\Delta G_m = \mathbf{R}\mathrm{T}\,[n_1 ln\phi_1 + n_2 ln\phi_2 + n_1\phi_2\chi] \qquad (2,23)$$

Here χ is known as the Flory-Huggins interaction parameter, the interaction parameter χ can be understood as an empirical parameter dependent on chain length and composition, in addition to temperature.

$$\chi = z \cdot \Delta\varepsilon_{AB}/kT \qquad (2,24)$$

Where z is the lattice parameter and ε_{AB} is the interaction energy between A-B pair, k is the Boltzmann constant. Thus χ is a temperature-dependent dimensionless quantity which characterizes polymer-solvent interactions and can be expressed more simply in the form:

$$\chi = a + \frac{b}{T} \qquad (2,25)$$

Where *a* and *b* are temperature-independent quantities. More generally, χ is given as the sum of enthalpy χ_H and entropy χ_S component.

$$\chi = \chi_H + \chi_S \qquad (2,26)$$

The equation (2.12) can also be converted to be the Gibbs free energy of mixing per mol of segments.

$$\Delta G_m^* = \mathbf{R}T\,[\phi_1 \ln \phi_1 + (\frac{\phi 2}{x}) \ln \phi_2 + \chi\, \phi_1\, \phi_2] \qquad (2.27)$$

Where $\phi 1$ and $\phi 2$ are the volume fractions of solvent and polymer, respectively. And x is the number of segments in each of the polymer molecules. The first two terms in equation 2.16 are from the combinatorial entropy of mixing and always are negative, thus promoting miscibility. The final term comes from the contact interactions and is positive. The temperature and χ will determine whether or not a polymer solution will phase separate. Thus, the ΔGm^* versus ϕ_2 curves can be considered to have these two general forms:

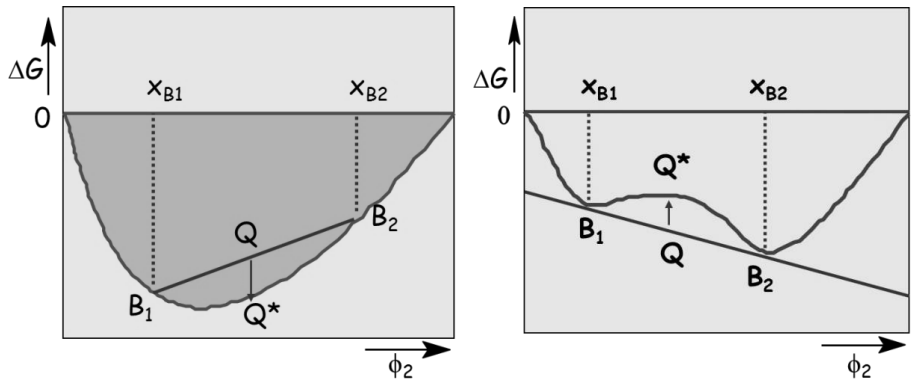

Figure 2-21: Two different phase behavior, miscible blends (left) and immiscible blends (right)

For the left graph, the polymer and solvent are miscible in all proportions, and it can be evidenced by the tie-line B_1–B_2. From B_1 to B_2, it is relatively simple to show that the Gibbs free energy change associated with phase separation process is given by the difference between (i) the value of ΔG_m^* corresponding to the point of intersection of the tie-line at *Q*, and (ii) the value of ΔG_m^* on the curve at *Q**, this difference is positive for all the points on the curve and so the existence of a single homogeneous phase is favored for all ϕ_2.[44]

For the right graft, we could see that the ΔG_m* versus ϕ_2 curve is rather more complex since two ΔG_m^* minima are present. For the range $x_{B1} < \phi_2 < x_{B2}$, the tie-line is joining two points below the curve, thus the homogeneous solution is unstable. When we consider this curve range more carefully, we can put shorter tie-line in different positions in the curve, which shows that the tie-line would rather above or below the curve itself. So here are some special points should be considered. At the two minima point which is when the two co-existing phases have the bimodal conditions, B_1 and B_2, can be described by the first derivative of the Gibb's free energy change on mixing with respect to composition:

$$\left(\frac{\partial \Delta G_m^*}{\partial \phi_2}\right)_{P,T} = 0 \qquad (2.28)$$

While the limit of stability (spinodal condition) is described by the second derivative of the Gibb's free energy change:

$$\left(\frac{\partial^2 \Delta G_m^*}{\partial \phi_2^2}\right)_{P,T} = 0 \qquad (2.29)$$

The critical point, which is the intersection of the spinodal and binodal curves, occurs when:

$$\left(\frac{\partial^3 \Delta G_m^*}{\partial \phi_2^3}\right)_{P,T} = 0 \qquad (2.30)$$

The existence of two minima in the variation of ΔG_m^* with ϕ_2 results from the contribution to ΔG_m^* due to contact interactions, which cause ΔG_m^* to increase. This contribution reduces as the temperature changes so the binodal and spinodal points get closer together until at the critical temperature which refer to the critical point. So based on this we can derive the T- ϕ_2 graph from the ΔG_m^*- ϕ_2 graph as the spinodal and binodal boundary change with temperature. [44](Figure 2-22)

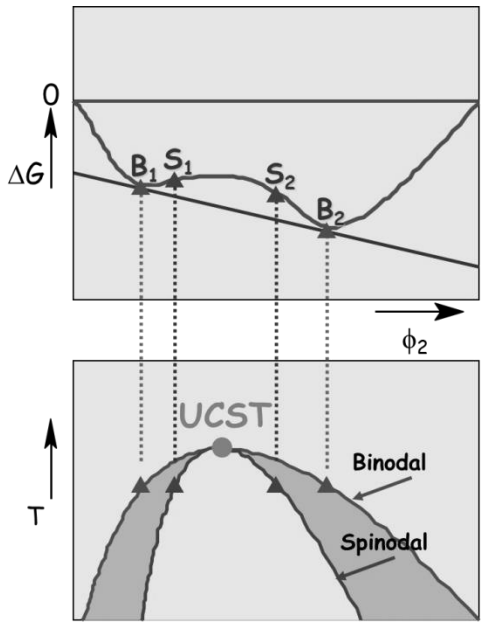

Figure 2-22: Derive the T- ϕ2 graph from the ΔGm*- ϕ2 graph as the spinodal and binodal boundary change with temperature.

The spinodal and bimodal boundary illustrate the stability of the system. The regions outside the bimodal correspond to stable homogeneous solutions, whereas the regions within the spinodal correspond to unstable solutions which will spontaneously phase separate. The regions between the binodal and spinodal correspond to metastable solutions which only phase separate if an energy barrier can be overcome.[44] The binodal boundary is a coexistence curve, where the system is at a local thermodynamic minimum and concentration fluctuation cease. The chemical potential equals in two phases, and clear solution starts to appear opaque. The metastable region between the two boundaries is where the phase separation proceeds by a process of nucleation and growth, like crystallization. The spinodal curve defines the regions of stability, so if a system is within the spinodal curve the system is unstable, and will spontaneously phase separate.

For most polymer solutions χ reduces as temperature increases, so that the critical temperature corresponds to the common maximum of the binodal and spinodal, and is known as the upper critical solution temperature (UCST), the polymer and solvent are miscible in all proportions when the temperature is above it. On the contrary, for the χ increase as temperature increases, is the critical temperature referred to be the lower critical solution temperature (LCST).

This section mainly explains the phase separation of polymer solution, and the derivation for UCST. But because of the neglect of 'free volume' concept, the Flory-Huggins theory couldn't predict the LCST behavior. The LCST phenomenon will be discussed more detailed later as it is the main mechanism of poly(N-isopropylacrylamide) perform as a temperature-sensitive polymer.

2.3.2 Lower critical solution temperature (LCST)

The lower critical solution temperature is a less common situation compared with UCST where χ increases as temperature increase, i.e. the contact enthalpy parameter b in equation 2.14 is negative, that the LCST phase separation is driven by unfavorable entropy of mixing.[44] In general, the unfavorable entropy of mixing responsible for the LCST can be explained from two physical origins. The first is associating interactions between the two components such as strong polar interactions or hydrogen bonds, which prevent random mixing.[45] A second origin of the LCST behavior is free volume effects, which is caused by volume contraction upon mixing, so at high enough temperature, the volume change on mixing is negative, resulting in decreased entropy.[44]

The LCST behavior caused by the free volume effects had been explained by D. Patterson.[46] It is clear that the temperature dependence is not predicted by the monotonically

decreasing χ *(T)* relationship given by equation 2.14, in the LCST behavior, it shows the contrary. For polymer solutions, due to the long chain lengths of polymers, the entropy of mixing polymers is relatively small compared to that of small molecules and oligomers. The enthalpy of mixing polymers can be negative.

The critical value of x is still given by the Flory-Huggins combinatorial entropy approximation:

$$x_c = \frac{1}{2}\left(1 + r^{-\frac{1}{2}}\right)^2 \qquad (2,31)$$

Where r is the ratio of molar volume of polymer and solvent. Thus χ, increases as the molecular weight of the polymer is decreased. Decreasing molecular weights of polymer therefore come out of solution at increasing temperature at the LCST.[46]

In the case of polymer solutions, the LCST also depends on polymer degree of polymerization, polydispersity and branching as well as on the polymer's composition.[45]

G. ALLEN[47] had discussed the relationship between molecular weight and LCST. He suggested that the molecular weight of the polymer affects the situation of a LCST in any particular solvent. Polymers of low molecular weight (about 10^4kD) undergo phase separation within 20 ℃ or 30 ℃ of the solvent's gas-liquid critical temperature, while polymers of high molecular weight (> 10^4kD) separate at temperatures as much as 120 ℃ below the gas-liquid critical temperature. He did the experiments for the effect of molecular weight on the LCSTs with three polymer-solvent systems: polystyrene + cyclopentane, polypropylene oxide + n-pentane and polyisobutene + isopentane. The results shown in Figure 2-23 for polystyrene + cyclopentane suggest that the LCST is more sensitive to molecular weight variation compared with the change of UCST.

Polystyrene $\bar{M}_v$	Critical temperatures of polystyrene solutions UCST (°C) in cyclohexane[8]	LCST (°C) in cyclopentane*
$1{\cdot}3 \times 10^6$	31·2	150
$2{\cdot}5 \times 10^5$	27·8	164
$8{\cdot}9 \times 10^4$	23·6	172
$4{\cdot}3 \times 10^4$	19·2	178

Figure 2-23: The effect from molecular weight for the UCST and LCST of polystyrene + cyclopentane system.[47]

2.3.3 Temperature responsive polymers

Functional polymers, which can react, adjust or modulate their physicochemical character in response to an external stimulus, are generally referred as stimulus responsive polymers (SRP), or "smart" materials, which represent one of the most exciting and emerging classes of materials.[48,49,50,51,52] Polymers act as one of the main groups of "smart" materials because they are cheaper and more easily tailored than metals or ceramics. These polymeric "smart" materials can respond to environmental stimuli including pH, temperature, ions, solvents, electrical fields, magnetic fields, light, pressure, chemical and biochemical compounds. In this way, the functional polymers consequently have a wide range of applications that include sensors, drug delivery, gene delivery and tissue engineering.[53,54]

Temperature is the most widely used stimulus among environmentally responsive polymer systems. As we have introduced above, one of the unique properties for temperature sensitive polymers is the presence of their critical solution temperature, which refers to the upper critical solution temperature (UCST) and lower critical solution temperature (LCST). LCST and UCST are the respective critical temperature points below and above which the polymer and solvent are completely miscible. For example, as we are focusing on the LCST

behavior, which shows that a polymer solution below the LCST is a clear, homogeneous solution while a polymer solution above the LCST appears cloudy.[48] This favorable phenomenon can be explained by the thermodynamics based on the Gibbs free energy and Flory-Huggins theory that were discussed above.

Thermoresponsive polymers can be categorized by their structure. The main form of this group of polymers are hydrogels, which are 3-dimensional polymeric networks that are dispersed in water and form semi solid states containing upwards of 99% water w/w to polymer. There are two types of hydrogels: physical gels and covalently linked gels, the latter are based on polymer chains that are linked together through covalent bonds at points which are called crosslinks.[55] Hydrogels can be categorized into small branches as:[48]

(1) Micelles, which combine hydrophilic and hydrophobic monomers into block copolymers allow the formation of ordered structures in solution, which are usually used in drug delivery.

(2) Cross-linked micelles, the formation of micelles in solution are a reversible and dynamic process; this can be overcome by crosslinking polymer chains once micellization has occurred.

(3) Interpenetrating networks, which consist of two covalently linked polymer networks that are bound together by physical entanglement as opposed to covalent bonds. Specifically, this requires the polymerization of both networks simultaneously and results in two intermixed networks that can only be separated by breaking bonds.

(4) Polymersomes, based on self-assembled amphiphilic block copolymers with a hydrophilic interior and exterior, which have often been used for DNA delivery.[56] (Figure 2-24)

(5) Film.

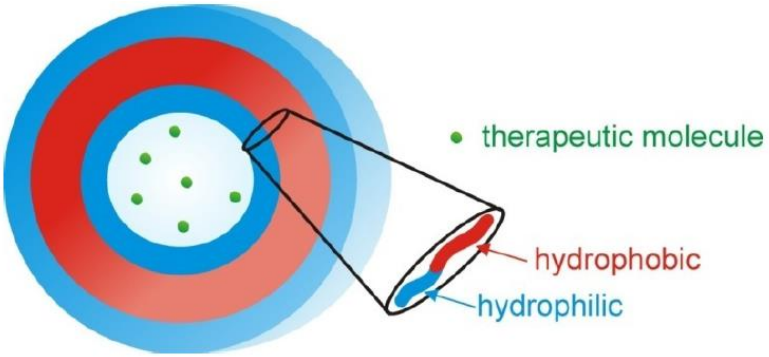

Figure 2-24: Polymersome formed by an amphiphilic diblock copolymer[48]

Most of the studies nowadays use polymers that present an LCST. For example the most common of this group of polymer is poly(N-isopropylacrylamide) (PNIPAM). PNIPAM has a lower critical solution temperature, LCST of around 32 ℃, which is a very useful temperature for biomedical applications since it is close to the body temperature (37 ℃). The LCST polymer will undergo a change of conformation at their LCST, when passing the LCST, the polymer chains collapse and display intramolecular hydrophobic interactions.[39] Here is a brief introduction for the categorization of LCST thermosensitive polymer:[39]

(1) Poly(vinyl ether)s. Figure 2-25 shows the structure for poly(vinylmethyl ether) (PVME). It could show the LCST in the physiological range, which is around 36 ℃ and is usually synthesized by living polymerization techniques.[57]

(2) Poly(N-substituted acrylamide)s. In particular of this group, poly(N-isopropylacrylamide) (PNIPAM) is the most known of thermoresponsive polymers having a LCST in the physiological range that is 32 ℃, (Figure 2-26). PNIPAM is easily prepared. It can be synthesized via free radical polymerization but also via controlled radical polymerizations.[39]

(3) Poly(N-vinyl caprolactam). This is another important thermosensitive polymer which has a LCST about 32-34 ℃. Poly(N-vinyl caprolactam) (Figure 2-27) is easily prepared by free radical polymerization of N-vinyl caprolactam in bulk or in solution.[39]

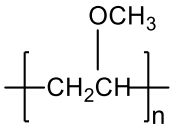

Figure 2-25: Chemical structure for poly(vinylmethyl ether) (PVME)

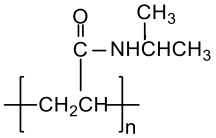

Figure 2-26: Chemical structure of poly(N-isopropylacrylamide) (PNIPAM)

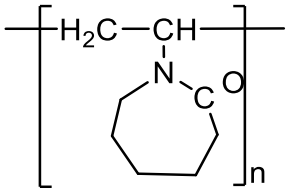

Figure 2-27: Chemical structure of poly(N-vinyl caprolactam)

Among all of the thermoresponsive polymers, poly(N-isopropylacrylamide) (PNIPAM) is the best known for wide applications. Shown in Figure 2-22, the repeating unit has both hydrophobic and hydrophilic moieties, therefore the aqueous polymer solution undergoes transitions between the water soluble state and the insoluble state depending on its degree of order at different temperatures.[39] PNIPAM undergoes the LCST at 32 ℃. Below the LCST, the polymer chains swell in water. The polymer chains exist as oils due to

hydrogen bonding of amide groups with water. Above the LCST, the solvent quality changes and the polymer segments are thought to become more hydrophobic, therefore the solution turns cloudy. (Figure 2-28) The mechanism of the behavior above or below LCST for PNIPAM can be explained by the connection or disconnection of the hydrogen bonds between water and amide groups from PNIPAM. In condition of low temperature, the hydrogen bonds between water and amide groups play an important role to make PNIPAM soluble in water as the polymer chains exist as oils. Above LCST, as temperature is higher, hydrogen bonds between water and PNIPAM will gradually breakdown, this is considered plausible that hydrogen bonding is weakened as the kinetic energies of the molecules become larger than the energy of hydrogen bonding between water and the molecules, where PNIPAM turns to be insoluble in water due to the hydrophobic isopropyl groups, and the solution turns to be cloudy because of the phase separation.

Figure 2-28: PNIPAM solution below LCST (left) and above LCST (right)

Also the extent of chain collapse above the LCST depends on both the grafting density and molecular weight. Chain collapse occurred at high grafting density and molecular weight.[58]

2.3.4 Temperature and pH induced phase transition behavior of copolymer of N-isopropylacrylamide and acrylic acid

Poly(N-isopropylacrylamide) (PNIPAM) is well known for its phase transition behavior as the temperature change around its LCST, which has a wide range of applications in drug-delivery[59], bioengineering[60] etc. But the important feature for PNIPAM/water is to modulate the LCST by a variety of techniques. This thermal-sensitive polymer with different LCST can be prepared by copolymerization with hydrophilic or hydrophobic comonomers.[61,62] Moreover, adding salts[63] or surfactants[64,65] into the PNIPAM/water solution are also effective for adjusting the LCST of PNIPAM. Karjalainen et al.[66] have prepared di-block copolymers of PNIPAM and polymerized ionic solution, they studied the effect of cationic structure of ionic solution on the thermal properties of PNIPAM. Jein et al.[40] have prepared a random copolymer of PNIPAM with different N,N-di-substituted imidazolium based ionic liquids and studied their LCST behavior.

Besides of the effect from comonomers, salt and surfactant, the polyelectrolyte is another representative solute to the thermal behavior of PNIPAM.[67] The ionizable groups in polyelectrolyte is sensitive to environmental pH.[68] Poly(acrylic acid)(PAA) is one of the pH sensitive polymer, whose degree of ionization of carboxylic acid groups is determined by the environmental pH. The combination of PAA and PNIPAM has been studied for their specific swelling and shrinking transform depended on both temperature and pH induced property.[69,70,71,67,72]

Chen and Hoffman[69,70] have studied the phase transition properties of both random copolymer of NIPAM and AA and graft copolymer of oligoNIPAM on a PAA backbone from a pH range 4 to 7. This copolymer not only has the bio-adhesive properties of PAA

copolymers depend on the densities of carboxyl groups, but also the thermal LCST transition properties of PNIPAM also depend on long sequences of homo-PNIPAM. It is known that:

(1). When the pH is higher than pK_a of PAA (around 4.7, depends on the conformation), the carboxylic groups are completely ionized.

(2). at lower pH, the non-ionized groups will form inter- and intra-molecular H-bond between PAA and PNIPAAM, which will hinder the water-PNIPAAM interactions. (Figure 2-29)

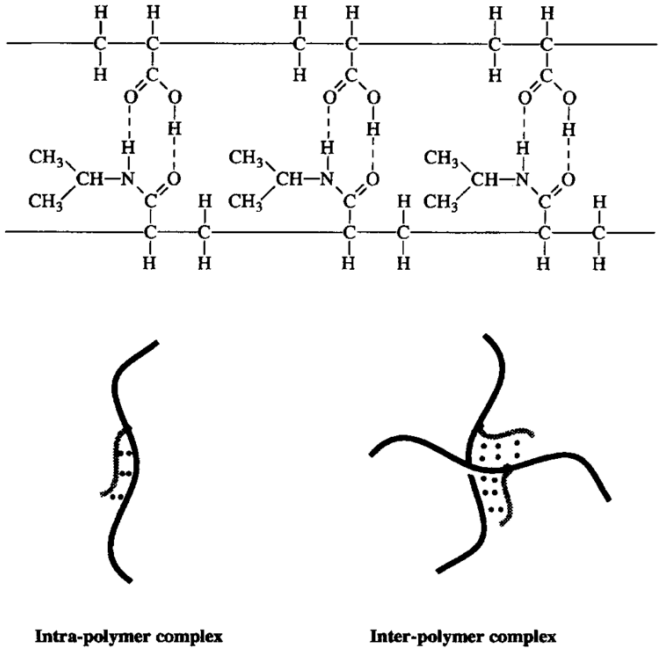

Figure 2-29: H-bonded complexes between the -COOH groups of the PAA and the -CONH- groups of PNIPAM.[69]

(3). by increasing the temperature, the non-ionized acid groups will become ionized and contribute to the hydrophilic properties of the copolymer.

For random copolymer, at pH=7, all acid groups are ionized, therefore, there is no LCST, because H-bonds are dominated by interactions between the acid groups with water, when % of PAA is higher than 10%; at pH=4, the acid groups are non-ionized. The LCST will

disappear when % of PAA is higher than 40%, because of inter and intra molecular H-bonds. Higher %PAA and lower pH will lead to lower LCST when $pH<pK_a$. For graft copolymer, the LCSTs are similar at certain pH with different %PAA. When $pH<pK_a$, which leads to lower LCST that caused by inter and intra H-bonds. Figure 2-30 shows the different LCST behavior between random copolymer and graft copolymer.

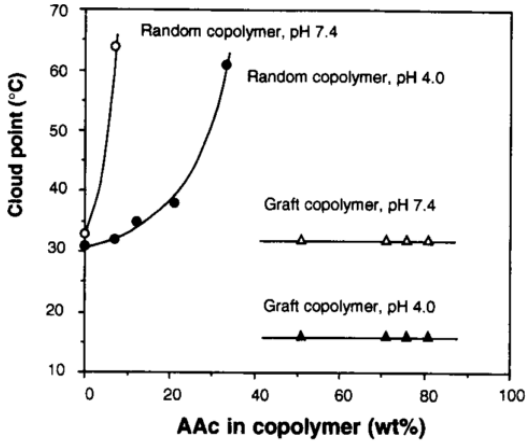

Figure 2-30: The phase separation cloud point of random copolymer and graft copolymer at pH 4.0 and pH 7.4[69]

Figure 2-31 shows 4 different stages of the hypothetical conformation of the copolymer under different pH. In region A, where the pH is above pK_a of PAA, and the temperature is below LCST of PNIPAM, the copolymers are at their most soluble and expanded conformation. When the temperature rises to region B, the PNIPAM chains independently phase separate due to the breakdown of the hydrogen bonds between PNIPAM and water. When pH is lower than pK_a and the temperature is below LCST, the acid groups in PAA are less ionized and inter or/and intra-molecular hydrogen bonds between PNIPAM and PAA will occur and the polymer chains will shrink but remain soluble as region D shows. At region C, both collapse of PNIPAM and hydrogen bonds within the copolymer will occur.

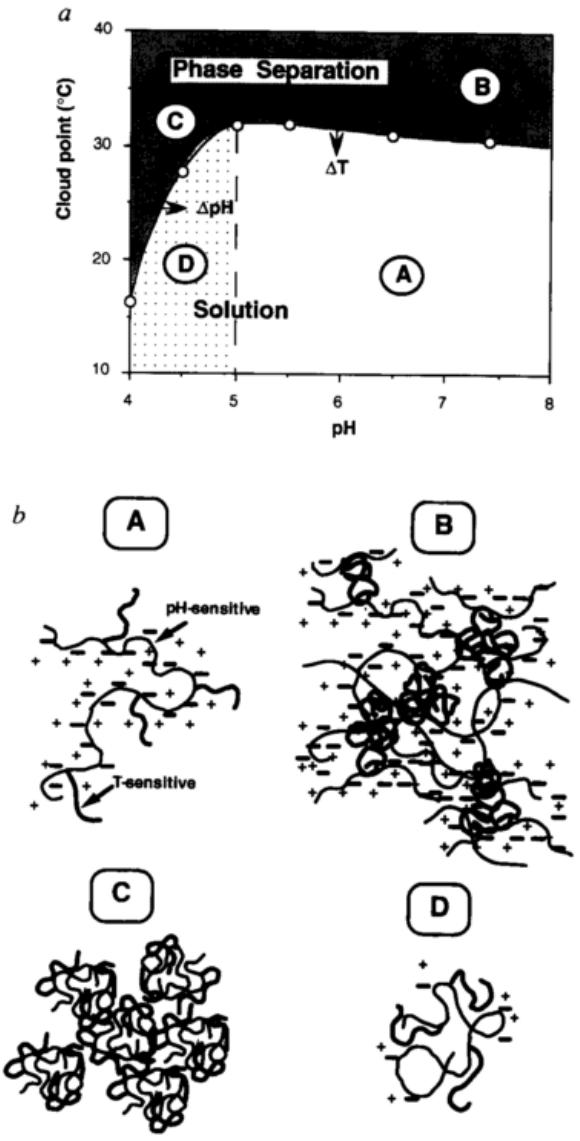

Figure 2-31: The cloud points of the graft copolymer (50%PNIPAM) versus pH, and the conformation of regions A-D, respectively.[69]

2.4 Summary of literature reviews

From the literature reviews above, the basic concept and mechanism of wetting and wicking have been explained, which provide the fundamental resources for this project. Also, based on the thermodynamic theory, the phase-separation and LCST phenomenon have been

introduced, which is critical for the design of dynamic moisture management systems. At the same time, surface characterization techniques and approaches to improve the surface of fabrics are also reviewed, which provides us information about how to modify the surfaces of the given commercial products.

3. EXPERIMENTS

3.1 Material and instrument

White, salmon and blue fabrics were supplied by Eastman. Poly(acrylic acid), (MW 450,000 g/mol), stearyl alcohol (1-Octadecanol), N-isopropylacryl-amide, ammonium persulfate, and N,N-methylene-bis-acrylamide were purchased from Sigma Aldrich. Reactive blue 19 was purchased from DyStar. Distilled water was obtained in-house.

The dip-pad process was carried out on a Werner Mathis AG padder. (Figure 3-1) The fabric was dried in a Yamato Scientific America Inc. oven (Figure 3-2) and cured in a Werner Mathis AG oven. (Figure 3-3)

The profiles of droplet on the surface were captured using a Meiji EMZ-13TR zoom stereomicroscope (Meiji Techno America, Santa Clara, CA) and Canon EOS camera (Canon USA, Inc, New York). The 10 μL microsyringes (Hamilton Company, Mircoliter 7002) were used to deposit droplets on the fabric surfaces. The contact angle was measured by E-scope® USB camera purchased from Amazon. The drying time was measured by AL54 analytical balance(Mettler Toledo, Schweiz) connected with software Putty. The content of PAA was measured by GENESYS 10S UV-Vis Spectrophotometer (Thermo Electron Corporation). And the shaking bath was purchased from Precision Scientific. The figures and analysis of the photos were done by Adobe Illustrator CS6, Image J, E-scope, JMP, Origin and Adobe Photoshop CS6.

Figure 3-1: Werner Mathis AG padder

Figure 3-2: Yamato Scientific America Inc. oven

Figure 3-3: Werner Mathis AG oven

3.2 Image analysis of wicking behavior on different fabrics

We developed and investigated two relative methods for image analysis of different fabrics. The image analysis aims to capture and describe the wetting and wicking behavior of little water droplets on different fabric surface under different magnification.

The first method for wetting and wicking area observation is by using camera connected with stereo microscope to capture the local wicking behavior along the yarns of three different fabrics under higher magnification. And also a regular photo capture of wetting area for three different fabrics which aims to compare the relative difference between these three. Each kind of fabric has been cut into small rectangular pieces about 1.5cm*3cm. 1μL water droplets were deposited on the surface of each fabric by using microliter syringe with measuring range of 10μL. Here, for better observation, we use reactive dye to color the wetting area. Reactive dye has great water solubility which could present accurate wetting and wicking process. Reactive blue 19 is used at a concentration of 6mg/mL in DI water. The

final wetting area with whole boundary was captured by camera. The local wicking behavior under higher magnification was captured by set up stereo microscope connected with camera as (Figure 3-4) shows. Fabric strip was deposited on a glass substrate.

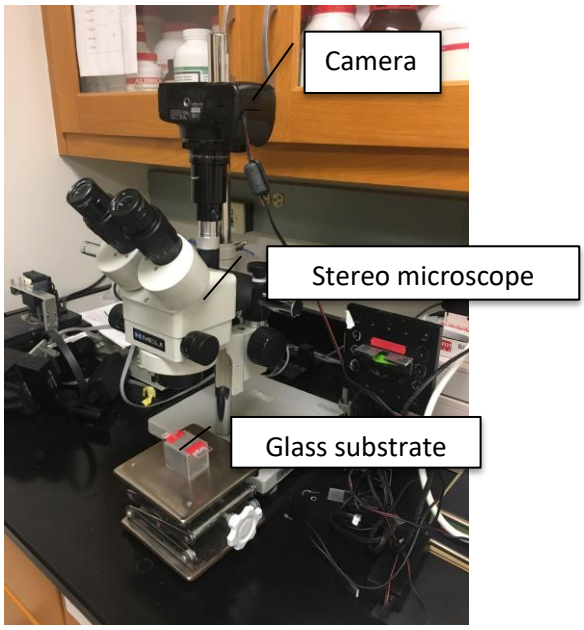

Figure 3-4: Camera connected with stereo microscope for image analysis

Another method uses a USB camera connected with e-scope software on computer to have photo and video captured. (Figure 3-5) The magnification of USB camera can be adjusted with different distance. The fabric was put on a glass substrate, and also the surface was deposited with 1μL dye water(10mg/mL). Photos with a 2 second time interval and videos for the whole wetting and wicking process until the wet boundary won't change have been captured. The video has been edited by using software Corel Video Studio and has quick screenshot at certain time point. Image-J was used for image analysis, measured the distance for both wale and course direction of wetting area.

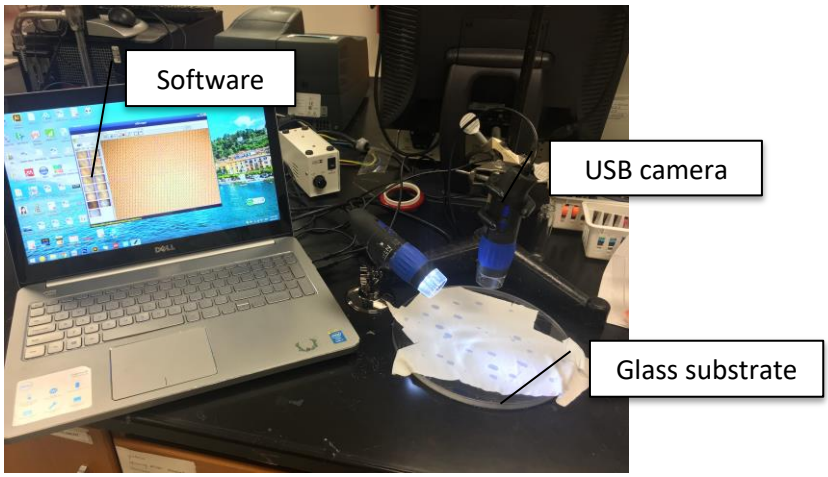

Figure 3-5: Image analysis by using USB camera

3.3 Dry time analysis of different fabrics

The dry time measurement is by using analytical balance connected with software Putty to record the drying time according to the weight loss from the water droplet deposit on the fabric surface until it was totally dry. It can be combined with the image analysis method with the drying process captured at the same time. The fabrics were cut into rectangular pieces and put in the container. Because of the sensitivity of the balance, no air flow was added for accelerating the drying process. 1μL of DI water was deposited on the fabric surface and the weight change was recorded by Putty. The data recorded by Putty is at constant time interval, which can be converted as 3 time points equals to 1 second. The data was analyzed using JMP.

3.4 MMT test.

AATCC 195 is a standard method by using moisture management tester (MMT) for the measurement, evaluation and classification of liquid moisture management properties of textile fabrics. Results obtained from this method are based on the water absorption and

resistance of fabric structure including the geometry of fabric and wicking characteristics of its yarns and fibers.

In order to measure the moisture management properties of textiles, fabric specimen should be placed in the moisture management tester (Figure 3-6) between two horizontal (upper and lower) electrical sensors each with seven concentric sets of pins.

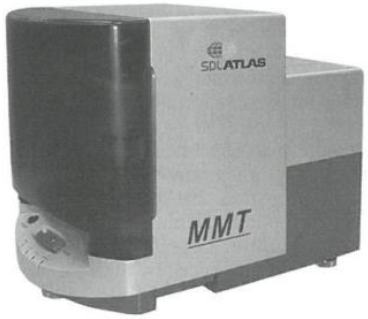

Figure3-6: Moisture management tester (MMT)

Fabric samples are cut into 8cm*8cm, at least 5 samples are needed for each trial in order to get average results. A predetermined amount of test solution is dropped at the center of test fabric surface. Test solution is prepared by dissolving 9 gram sodium chloride in 1L of DI water. The standard solution pump volume is 20 μL, and the 'measure time' is 120 seconds. During the test, changes in electrical resistance are measured and recorded. The electrical resistance is used to evaluate the moisture transport behavior in different directions, which are summarized as absorption rate for upper and lower surface, accumulative one-way transport capability, maximum wetted radius, total water content and overall moisture management capability.

3.5 GATS test

The Gravimetric Absorbency Testing System (GATS) is used to measure the ability of the sample to take up liquid spontaneously in the direction perpendicular to its plane. It can accurately measure liquid absorption rates and total capacity. Demand wettability is measured by the amount of water drawn from a water filled reservoir. During testing, water absorbed by the test specimen is re-supplied through a tube that connects to the porous test plate. The GATS instrumentation is pictured in Figure 3-7:

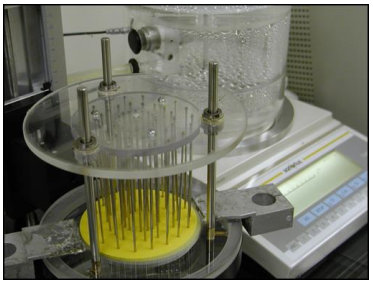

Figure 3-7: GATS instrumentation.

Circular samples were prepared with diameter of 3.5in. Absorption parameters have been measured including:

Wd: dry weight of the conditioned sample specimen, grams

Ww: wet weight of the sample specimen at the end of the test, grams

V: amount of water passed from the reservoir during 1000 seconds, grams

T: time, minutes. This is the point where the extrapolated absorption and evaporation areas of the curve intersect.

And we mainly look into the absorbent capacity, which refers to the amount of water contained in the sample at the end of the test.

3.6 PAA pre-treatment on polyester woven and knit fabric surface

Poly(acrylic acid) was first grafted on the surface of polyester fabrics for pre-treatment because it contains high functional side groups. Once it formed covalent bonds to the fiber surface, it could introduce many carboxylic acid groups for further reactions. Both woven fabric (white) and knitted fabric (black) were prepared with sample size of 10cm*15cm.

The white woven fabrics were used for pre-experiment, in order to check the feasibility. In the pre-experiments, the padding aqueous solutions (3% ~5%) were prepared by dissolving PAA in distilled water under high speed stirring. The temperature for stirring is around 30℃ for better and quicker dissolving. The surface treatment was followed by the pad-dry-cure procedure introduced in literature review part 2.2.5. Fabric samples were dipped into the solution 1-2 times and then padded using the padder (Figure 3-1), with feeding speed of 1m/min and linear pressure 1N/cm^2. Then the padded fabrics were dried in the oven (Figure 3-2) for 30s at 50℃ in order to evaporate excess water. Finally, samples were cured in another oven (Figure 3-3) at 175℃ with different curing time from 1-3 min. By measuring the moisture management properties for treated fabrics, the best treated condition will be concluded for further experiment use.

The black knitted fabrics were used as the main experiments for this study. The grafting methods were same with pad-dry-cure procedure as introduced above. The concentration of PAA aqueous solution was prepared as 2%, and the cure time was 2 min.

3.7 Create hydrophobic yarns within polyester woven and knit fabric

In order to render the interior of the yarn hydrophobic, a long chain aliphatic alcohol, stearyl alcohol, was attached to the PAA treated fabric. The same procedure was followed by pad-dry-cure to graft stearyl alcohol onto and into the fabric. In the pre-experiment with woven fabric, different concentrations of stearyl alcohol aqueous solutions from 1-3% have been prepared under high stirring speed at 70 ℃. (The melting point of stearyl alcohol is 59.4 ℃ -59.8 ℃) The padding process should be finished while the solution remains at high temperature, because stearyl alcohol is not soluble in water below its melting temperature. The drying process can be omitted in this treatment. Curing was carried out at 175 ℃ for 3 min. For knitted fabric, the concentration of solution was used as 1.5%.

For procedure optimization, experiments 3.5 and 3.6 can be combined into one procedure for higher efficiency. The aqueous solution contained 2% PAA and 1.5% stereo alcohol and stirred with high speed at 70 ℃. The curing section was carried out at 175 ℃ for 2 min. Samples after treatment were washed and dried with airflow.

3.8 Synthesis of the moisture management copolymer

Poly(N-isopropylacrylamide) (PNIPAM) is synthesized followed by this recipe. 2.00g NIPAM and 60mg of BIS were dissolved in 50mL filtered, deionized water in a three-neck flask equipped with a stirrer and purged with nitrogen for 20 min. The liquid was heated to 80℃ and the polymerization was initiated by addition of 0.2g APS dissolved in 2mL water. After about 5 min, the solution started to become turbid and the reaction was continued for 30 min. The colloidal suspension was cooled rapidly below room temperature in an ice bath.

The hydrogel was filtered, washed in water several times and dried. The hydrogel was immersed in water and stored at cold temperature.

The copolymerization with 2-aminoethyl methacrylate (AEMA) was synthesized by replacing BIS to same mole about 64.4 mg of AEMA monomer. The copolymer solution was cooled down in ice water and stored at low temperature.

3.9 Attach 'smart' wetting technology on the fabric surface

The copolymer P(NIPAM-co-AEMA) aqueous solution was attached on the PAA and stearyl alcohol treated fabric, still followed by pad-dry-cure process. The cure temperature was reduced to 150 ℃ and lasted for 1.5 min.

3.10 Contact angle measurement

We have introduced the basic concept of contact angle in the literature review part, which based on the Young's equation: (Equation 2.5)

$$\cos\theta = \frac{\gamma_{SG} - \gamma_{SL}}{\gamma_{LG}} \qquad (2.5)$$

The contact angle was measured by using USB camera connected with software on laptop as shown in Figure 3-7: The fabric samples were prepared as 1.5cm*3cm, and adhered smoothly to the boundary on the glass substrate. The water droplet, about 5μL, was dropped at the edge of the fabric sample. Photos or videos were recorded by the software.

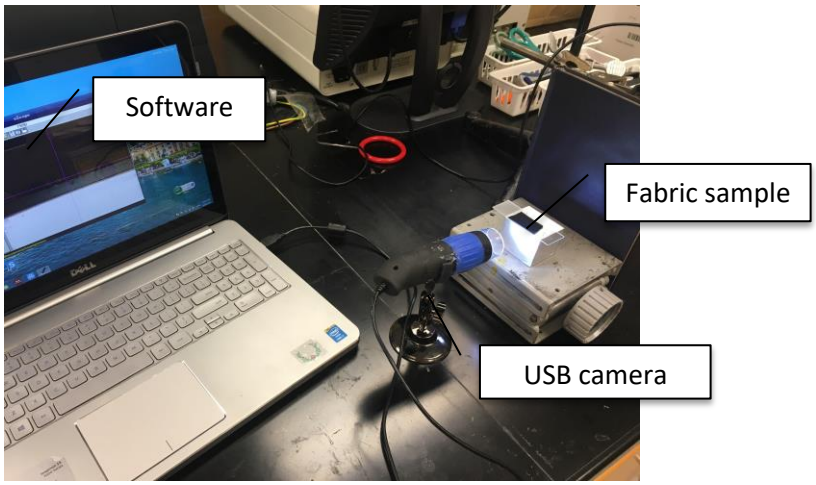

Figure 3-8: Contact angle measurement.

Then we used software, ImageJ and Adobe Photoshop CS6, to determine the contact angle. It is clear to estimate the wetting properties of the surface based on the contact angle, whether it is hydrophilic or hydrophobic.

3.11 Wet pick-up measurement

In order to determine the amount of chemical that ends up on the fabric, the wet pick-up (WPU) had to be determined. WPU is the percentage increase in weight of the sample after it has been padded and can be calculated as shown in Equation 3.1 below.

$$WPU = \frac{Wet\ weight - Dry\ weight}{Dry\ weight} \qquad (3.1)$$

Where:

WPU = Wet pick-up

WetWeight = Weight of wet fabric (grams)

DryWeight = Weight of dry fabric (grams)

After measure the weight of dry fabric, the sample will be dipped in the water and squeeze out extra water by padding with paper tower, and then measure the wet weight of fabric.

3.12 Drying rate measurement (AATCC 201)

The AATCC 201 standard test, also called heated plate method, which determines the drying rate of a fabric, exposed to a prescribed volume of water, while in contact with a heated plate set as 37 ℃, the skin surface temperature at which the human body starts to perspire. This method can be applied to all types of fabrics, including knits, wovens and nonwovens.

The drying rate is determined based on the evaporative rate that occurs when the fabric is placed in contact with certain amount of water at the interface with the heated plate, hold to a constant temperature. 3 specimens should be cut as 15cm*15cm for each trial of measurement. 0.2mL water will be applied on the plate below fabric sample as the device start to record data. The start time, which is the time when water has been attached to the specimen; and the end time, when the temperature goes back to the original temperature after the evaporation process, should be recorded. Drying rate is calculated by using this equation:

$$R = V/Drying\ rate \quad (3.2)$$

Where:

R= drying rate, in mL/h.

V=volume of water, in mL.

Drying time= End time- Start time.

3.13 Measuring PAA content on treated surface

The PAA contents on both two treated fabrics have been measured, which are the one grafted with PAA and the one grafted with PAA and stearyl alcohol.

30 μM stock solution of TBO was prepared by dissolving 0.0090 g of the dye in 1000 mL

deionized water. The solution was adjusted to pH=10 using 1 M NaOH solution. This 30 μM solution was labeled as C1. Serial dilutions were prepared based on C1 to get the standard curve. 15 μM(C2) was prepared by taking 50 mL C1 and diluting to 100 mL using pH=10 NaOH solution. 7.5 μM (C3) was prepared by taking 25 mL C1 and diluting to 100mL using pH=10 NaOH solution. 3.75 μM (C4) was prepared by taking 12.5 mL C1 and diluting to 100 mL using pH=10 NaOH solution. Each concentration was measured 4 times using cuvettes at 633 nm in GENESYS 10S UV-Vis spectrophotometer. The average of the four measurements was then used to prepare the standard curve of the absorbance versus dye concentration. The blank was pH=10 NaOH.

In order to measure the amount of poly(acrylic acid) grafted onto the surface of fabric, 0.1 g samples of the PAA grafted fabric were immersed in 20 ml (excess) of the 30μM(C1) TBO solution and left for treatment for 6 hours at 37 ℃ under constant agitation(30 Rpm) in the shaking bath, which allowed for the formation of ionic complexes between the carboxylic groups of the grafted poly(acrylic acid) chains and cationic dye. After 6 hours, the samples were removed and washed thoroughly with excess pH=10 NaOH solution to remove unattached cationic dye molecules from the samples. The washed samples were then placed in 20 mL of 50% (w/v) acetic acid solution for 30 min at 37 ℃ with constant agitation (30 rpm) in the shaking bath. This step allowed for the dye molecules on the fabric surface to diffuse into the solution. The TBO is released into the acetic acid solution and colored the solution blue. Then each blue solution was measured 3 times at 633 nm in GENESYS 10S UV-Vis spectrophotometer. 50% (w/v) acetic acid was used as the blank.

In order to compare the PAA content after grafted with stearyl alcohol, same procedure was carried out as introduced above using 0.1g sample of PAA with stearyl

alcohol treated fabric.

The same procedure was carried out for the control samples where no poly(acrylic acid) was attached.

4. RESULTS AND DISCUSSIONS

4.1 Wicking behavior of different fabrics

Three different fabrics provided by Eastman with the same knitted structure have been studied on their moisture transport behavior. The moisture transport behaviors differ, which is caused by the morphology difference of the yarns. All fabrics have been treated with wicking agent but still show significant different wetting behavior. The difference between these three fabrics is the type of yarn as shown in Figure 4-1:

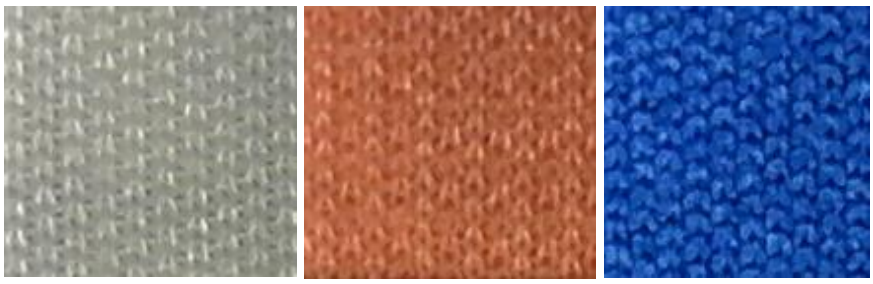

A B C

Figure 4-1: Three different fabrics as A(white), B(salmon) and C(blue)

White fabric is composed of 100% Eastman Avra™ Performance Fibers (polyester), salmon fabric is composed of 77% Avra™ filament yarns with 23% commercial polyester filament yarns, while blue fabric is made of 100% polyester yarns. The Avra™ filament yarns have special morphology as the cross section of fibers has a very high surface-to-weight ratio, and is much smaller compared with polyester yarns, which significantly enhances the wicking and drying behavior. Even with the same knitted structure and similar packing density, these three fabrics show totally different wetting behavior because of the yarn component. So we investigated the wetting behavior of these three fabrics by image

analysis, drying time measurement and standard moisture property measurement by using moisture management tester (MMT) and GATS.

4.1.1 Image analysis

The image analysis method is supposed to have a clear and better observation of wicking process under higher magnification, and also to capture good image and video, which could give us a better understanding of the wicking behavior within the fabric. We have proposed and set up two different image analysis devices for different use. The camera connected with stereomicroscope is for higher magnification observation, which could provide us a stable and bright image, and concentrate on specific local area. The other one is by connecting USB camera with video record software, to have continues image data. When we deposited 1 μL of water with dye on each fabric, the final wetting area is different as Figure 4-2 shows.

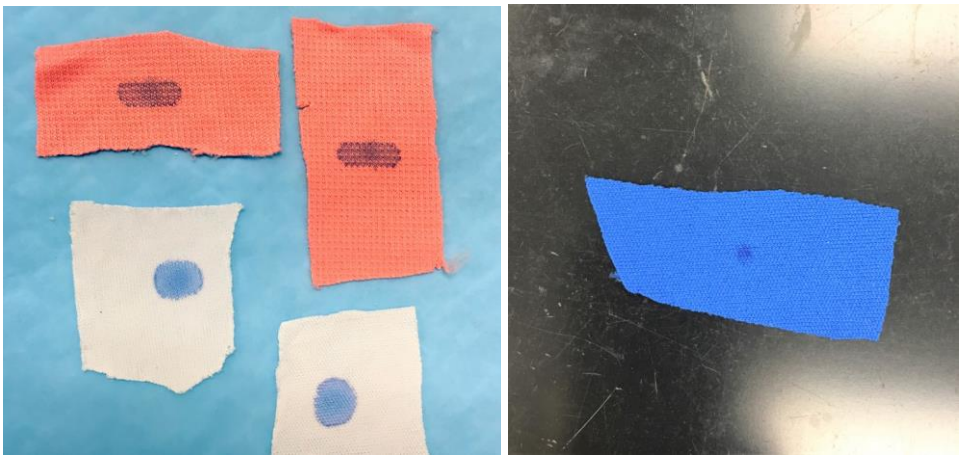

Figure 4-2: Different wetting area of white, salmon fabric(left) and blue fabric(right)(1μL)

We used Reactive blue19 dye for clear observation, and there is little difference between with dye and without dye which should not have an influence on image analysis. In Figure 4-2, the wetting area on white fabric has a round shape, however, on the salmon fabric

it is a long strip. Compared with these two fabrics, there is little wicking within blue fabric, whose wetting area doesn't change a lot from when droplet is deposited on the surface. This is because the polyester yarn has less moisture transport property than Avra™ yarns based on their fiber morphology. The smaller cross section of Avra™ fiber leads to higher capillary pressure, and the high surface-to-weight property can enhance the interaction with water as well. What we found interesting is that, the 23% yarn blend fabric has shown different wicking behavior, the 23% hydrophobic polyester yarns have played an important role in this process.

As we zoom in the wetting area of each fabric, we could see different color level for the area, this phenomenon has also been captured by Konopka's work.[73] We have simplified this model as shown in Figure 4-3:

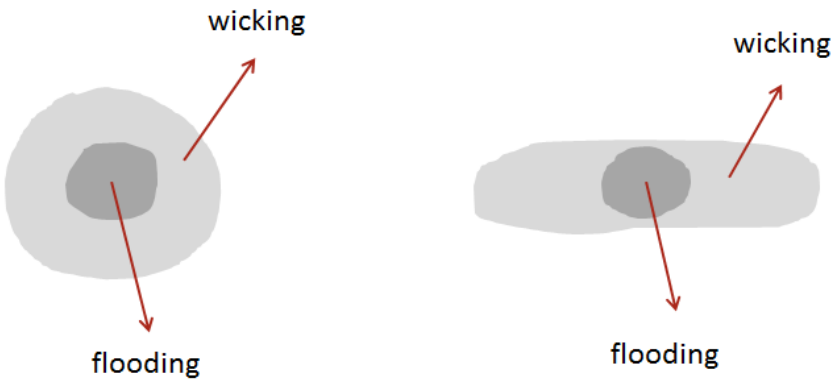

Figure 4-3: Different color level of wetting area for white(left) and salmon(right) fabrics

This can be explained by the flooding and wicking phenomenon. When water droplet is placed on the fabric, there is an initial stage called 'flooding' followed by the wicking process. Flooding is after water has been placed on the hydrophilic fabric surface, the liquid water will spread into the spaces between yarns in the knit or woven fabric. This phenomenon happens instantaneously as the contact angle decreases to 0 degree quickly. The

wicking process follows immediately to provide active transport of water though open spaces between fibers within the yarns. Compared with flooding, wicking will take longer time because of the tiny spaces.

The salmon wetting area has little wicking along perpendicular direction, which corresponds to the wales direction of knit fabric. Water mainly wicks along horizontal direction which is the course direction of knit fabric. According to the yarn component of these two fabrics, salmon fabric is the blend of Avra™ yarns with polyester yarns. We captured this area under higher magnification as shown in Figure 4-4 and Figure 4-5 for both white and salmon fabric respectively.

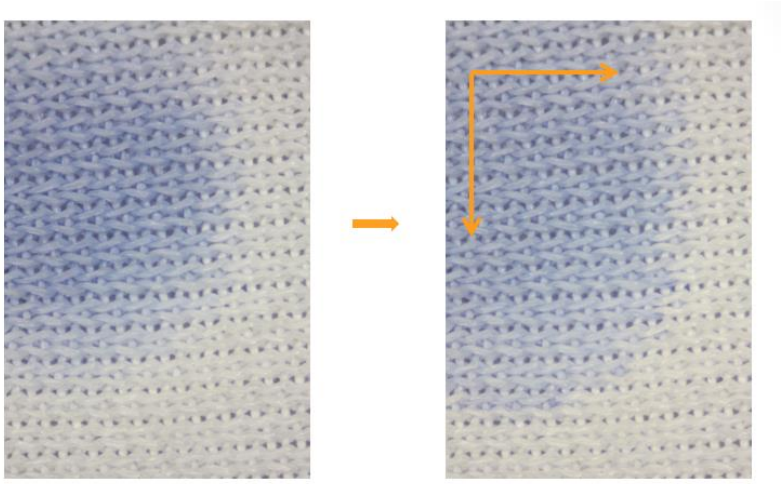

Figure 4-4: Wicking along white fabric

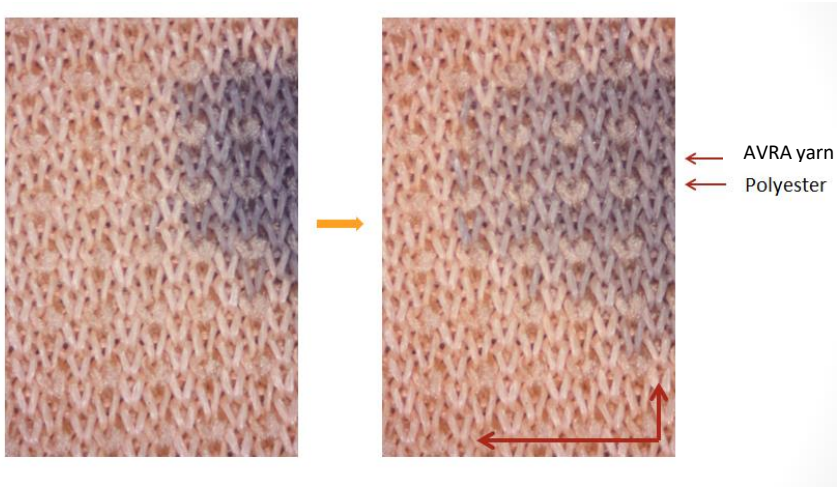

Figure 4-5: Wicking along salmon fabric

By comparing the wicking process of these two different fabrics, we found that the hydrophobic polyester yarns have played an important role in this process. White fabric is composed of 100% Avra™ yarns and has even wicking area. Water spread along all directions with similar speed along wales and course direction as a circle. But for salmon fabric, under higher magnification, we could see clearly that the fabric is blend with Avra™ yarn and polyester yarn as different wicking sequence along course direction. Polyester yarn has weak moisture transport property, but Avra™ yarn is much easier to wick, which resisted the wicking along wales direction, from Avra™ course to polyester course. In this case, the difference of wetting area between white and salmon fabric can be explained.

USB camera is used for video record for the wicking process of each fabric. We use quick screenshot for the video at different time points. Most photos are captured during flooding and the beginning of wicking stages as wetting area increased quickly during this period. After the wicking speed become constant, several photos were captured at certain time points. Photos are given in appendix as reference. We measured both wale and course

direction for each point of wicking process, for the blend fabric, we also recorded the course direction for PET yarns additionally.

Figure 4-6 shows the spreading distance with time change, for both wale and course direction of white fabric. Liquid in wale and course direction all flood quickly at the beginning, and then followed by the wicking process at a slow constant rate. Liquid in wale direction floods more than in course direction at the beginning as it depends on the knit structure, but as the wetting area has reached its final boundary, the distance for wale and course direction are similar within the rage of 200-250 pixel. So the final shape of wetting area is a circle.

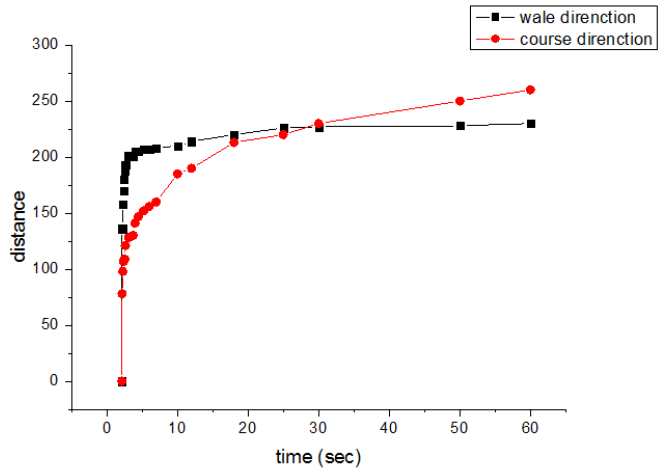

Figure 4-6: Spreading distance of white fabric

Figure 4-7 shows the spreading distance with time change for salmon fabric, and the course direction of PET yarns has been measured additionally. After the quick flooding stage, there is little wicking along the wale direction, which has been explained before, the polyester course will hold water wicking from Avra™ course. Water mainly wicks along the course direction with high spreading rate. Compared with wale direction wicking, the

distance of course direction is twice as fast as in the wale direction. The final shape of wetting area is a long strip rather than a circle.

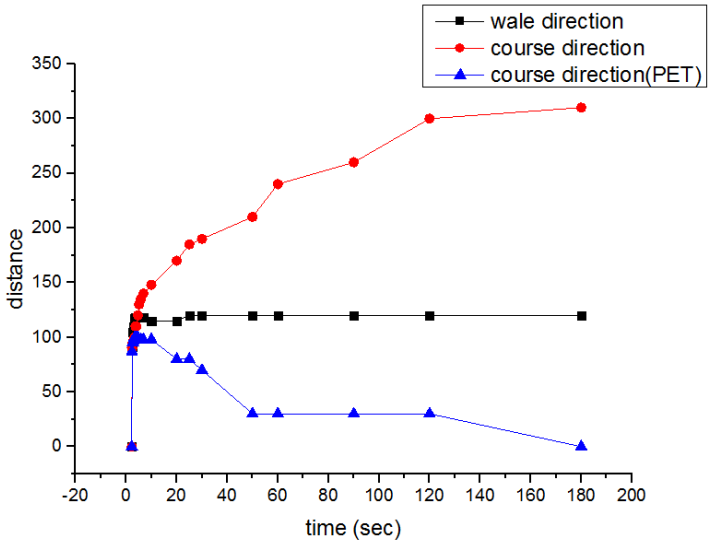

Figure 4-7: Spreading distance of salmon fabric

Another interesting phenomenon is that, from the data, wicking along course direction for polyester yarn decreases after the flooding stage. Figure 4-8 has shown the difference between the beginning and end of wicking for salmon fabric. The dye color in the polyester course has decreased with time change, as the color shows from darker to lighter. It indicates that the liquid has moved out of the polyester yarns during the wicking process. Water has been pulled out from polyester yarns because the Avra™ yarns around are more attractive to water. Water moves from polyester yarns to Avra™ yarns has contributed to the wicking distance along course direction. As there is no more liquid in polyester yarns, the wicking process for this whole area will reach to the final boundary gradually.

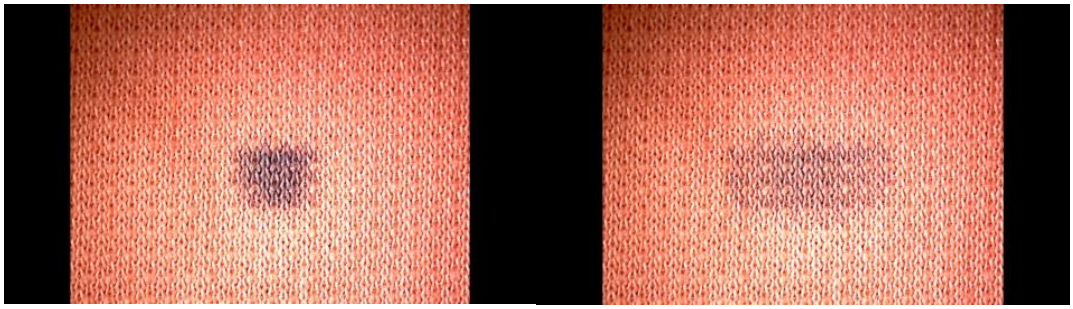

Figure 4-8: Different wicking stages of salmon fabric

The different hydroscopicity of PET and Avra™ yarn will definitely influence the wicking phenomenon of the fabric. As we compared the data between white and salmon fabric, the time for wicking to reach the constant level is different, and it can also be concluded from the video. The final wicking boundary shows at around 60 seconds for white fabric, while for salmon fabric it shows up around 180 seconds. During flooding and wicking stages, the slow evaporation of water happens at the same time. The larger the area and the earlier the final wicking area arrives, the faster the fabric will dry. So the white fabric with 100% Avra™ yarns dries faster than the blend salmon fabric. Furthermore, the blue fabric composed with 100% polyester dries even slower than the others, because of the smaller wetting area and little wicking process. This is discussed further in drying time analysis.

We also tried with larger volume of liquid (12 μL) on the surface. The wetting area showed in Figure 4-9 indicates that the difference of wetting area between white and salmon fabric has become smaller, the area in salmon has more like a circle rather than the long strip. This changes when depositing a larger volume of water and will also influence the drying time of these two fabrics.

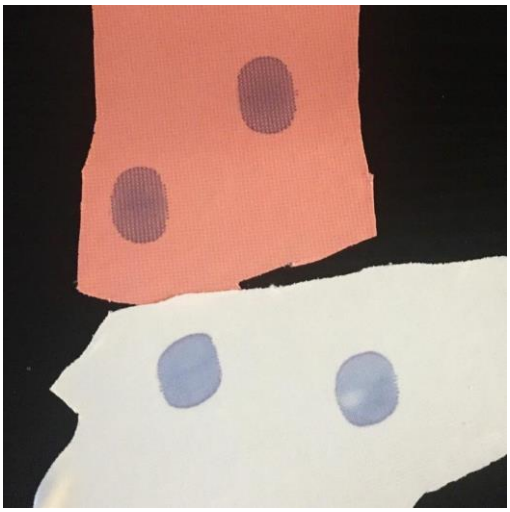

Figure 4-9: Different wetting area of white and salmon fabric (12μL)

4.1.2 Drying time analysis

The drying time is measured by using an analytical balance connected with software Putty to record the drying time according to the weight loss from the water droplet deposit on the fabric surface until it is totally dry. 1μL of DI water was deposited on the fabric surface and the computer started to record the weight change. The data recorded is at constant time intervals, which can be converted as 3 time points equals to 1 second. Figure 4-10 shows the drying time for three different fabrics.

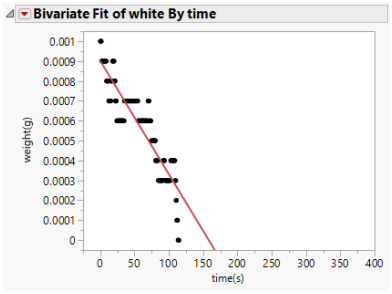

(a)

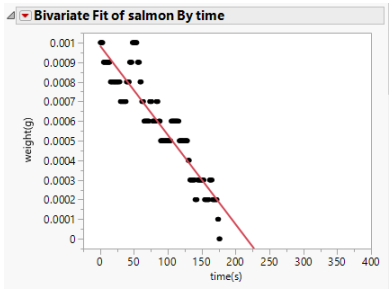

(b)

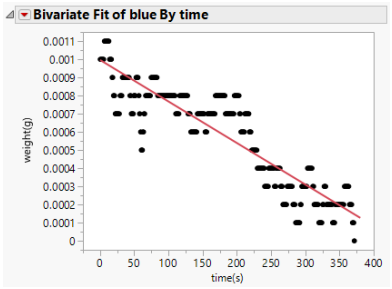

(c)

Figure 4-10: Drying time of three different fabrics (1μL)

The data shows that among these three fabrics, the white fabric has shortest drying time about 125 seconds and followed by salmon fabric with 175 seconds, blue fabric dries much slower than the others with up to 375 seconds. This is also corresponds to the deduction in image analysis that with quicker wicking process, white fabric can dry faster. Blue fabric needs longer time for drying because of the PET yarns. The drying time can be fitted with a linear fit, which shows different drying rates of these fabrics.

Figure 4-11 shows the drying time when 12 μL of DI water had been dropped on the surface.

With a larger amount of water, the difference of drying time between white and

salmon fabric has become much smaller. However, the blue fabric still dries slower than the others.

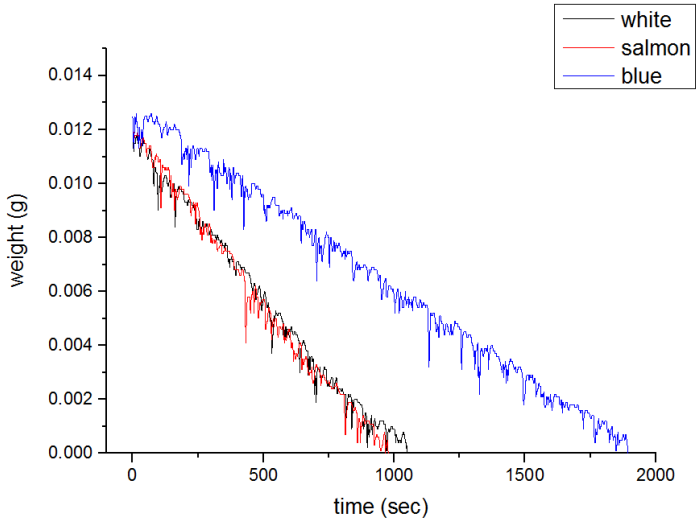

Figure 4-11: Drying time of three different fabrics(12μL)

4.1.3 MMT test

AATCC 195 is a standard method by using moisture management tester (MMT) for the measurement, evaluation and classification of liquid moisture management properties of textile fabrics. The standard solution pump volume is 20 μL, and the 'measure time' is 120 seconds. During the test, changes in electrical resistance are measured and recorded. The electrical resistances were recorded by the electrical sensors each with seven sets of concentric pins.(Figure 4-12) The wetting area will be shown as different level of blue color from dark to light, correspond to the moisture content.

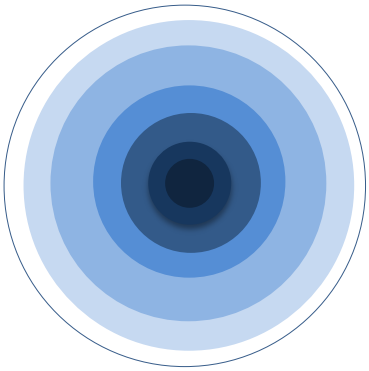

Figure 4-12: Different content of moisture measured by electronic sensors

The disadvantage for using MMT method to evaluate the wetting radius is that it can just present relative circular range, but not the actual wetting area, which would cause big error. For example, the salmon fabric has long strip wetting area, which could not be explained using MMT method. So the image analyzis for salmon fabric was more accurate and visualized for studying the wetting behavior.

Three fabrics, white, salmon and blue have been tested with MMT by running different pump times (12s, 5s, 1s) correspond to the pump liquid volume as 12μL, 5μL and 1μL respectively. Tests with 12s and 1s have been mainly concentrated on as it represented the wetting behavior for relatively large and small liquid volume. The one-way transport capability and relationship between water content increased with time have been studied. The One-way Transport Capability (%): R, which is the difference of the accumulative moisture content between the two surfaces of the fabric, has been measured for all three fabrics with three different pump times. (Table 4.1)

$$R=[\text{Area}(U_B)-\text{Area}(U_T)]/(\text{Total testing time}) \quad (4.1)$$

where:

U_B = the total water content of the bottom surface, and

U_T = the total water content of the top surface.

Table 4.1: The One-way Transport Capability (%) of three fabrics with different pump times

	12sec	5sec	1sec
white	138.8%	75.4%	29.5%
salmon	118.2%	61.8%	20.8%
blue	169.4%	109.4%	5.5%

The One-way Transport Capability has given us a vertical aspect for the wetting behavior. With large liquid volume(12μL, 5μL), the blue fabric showed higher R compared with the others, the salmon fabric had slightly lower R than white fabric. This can be explained that blue fabric is composed by hydrophobic polyester yarns, there is little wicking within the yarns, water mainly floods into the spaces between the yarns after water is dropped on the surface. Thus, the blue fabric has smaller wicking area but higher one-way transport capability. But for the tiny liquid droplet (1μL), blue fabric shows the lowest capability, which can be explained that liquid was held by the hydrophobic yarns, with small wicking area and water transport. But white and salmon fabrics composed of hydrophilic yarns have higher capability, which is because they have better wicking properties. Water could spread longer and led to faster evaporation.

Figure 4-13 to 4-16 shows the water content changes with time for white and blue fabric with 12s and 1s pump time. The tester is almost closed where little evaporation occurs inside, so the curves shown below cannot describe the evaporation process, rather wetting, flooding and wicking are the main processes that occur here. A small droplet has faster flooding where it shows vertical slope at the beginning, the flooding process for large droplet has been measured by the circular sensors gradually. For the wicking process, which

corresponds to the flat period on the curve, the blue fabric has little change of water content compared to the white fabric, which indicates that it is difficult for it to dry. And the flooding process for blue fabric with 1s pump time is slow, which indicates the smaller wetting area and less hydrophilic properties of blue fabric.

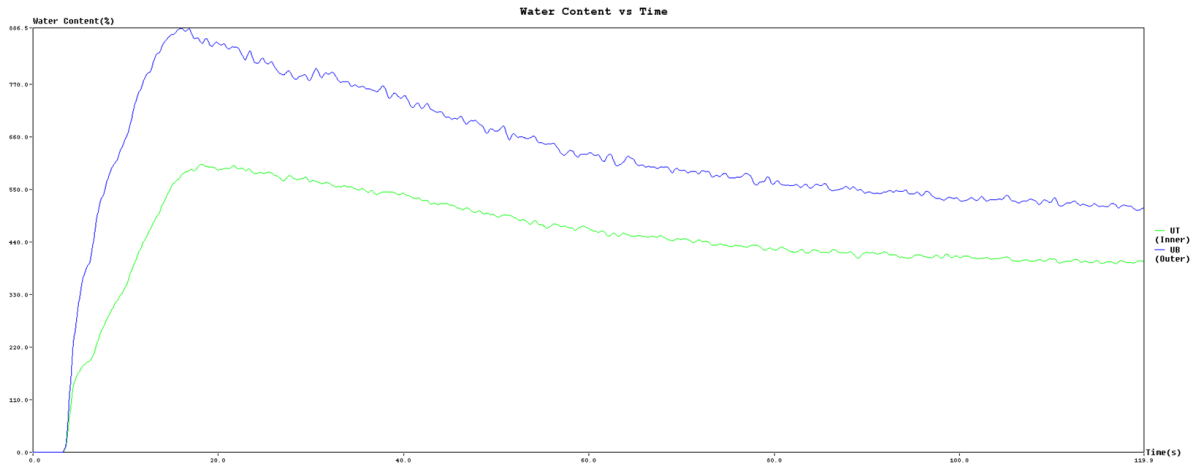

Figure4-13: Water content vs time of white fabric (12s)

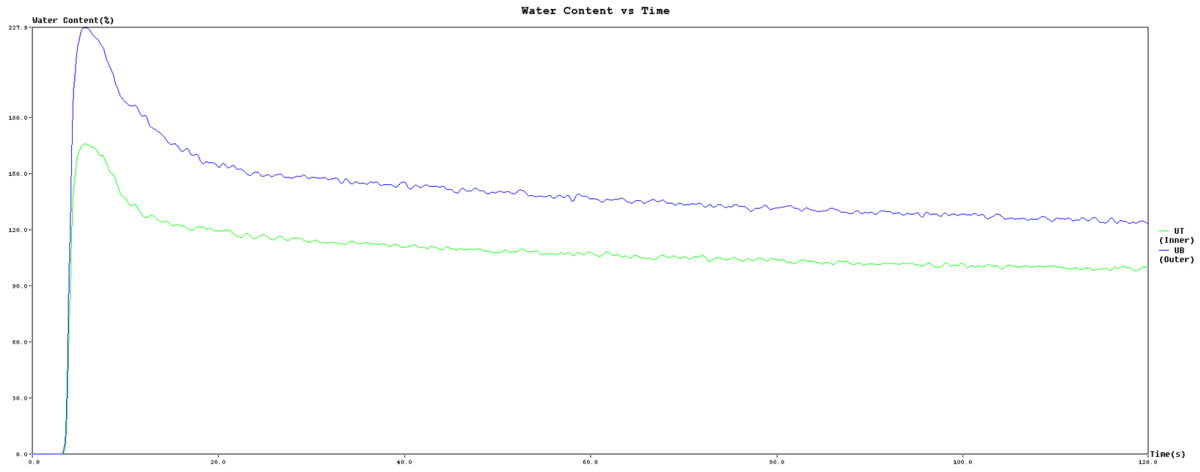

Figure4-14: Water content vs time of white fabric (1s)

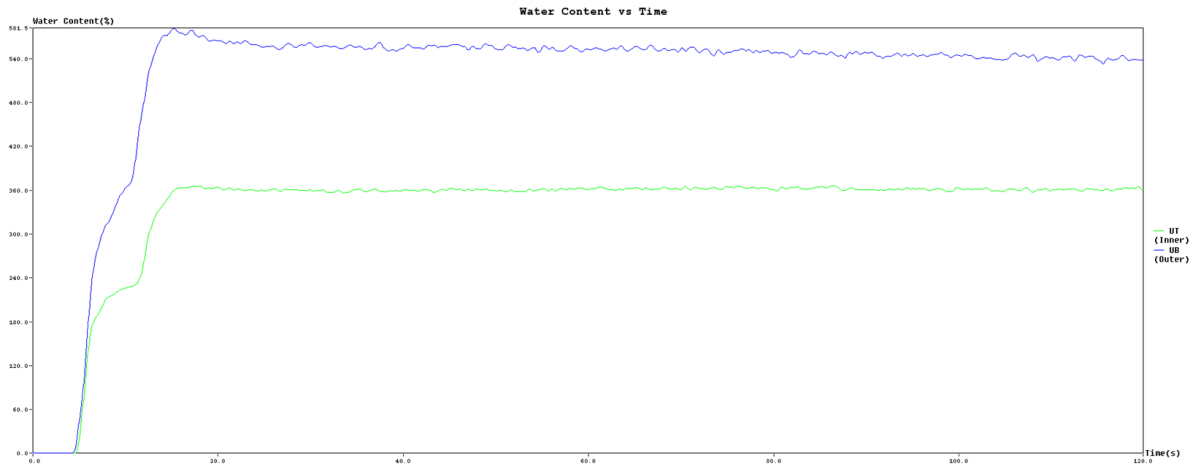

Figure4-15: Water content vs time of Blue fabric (12s)

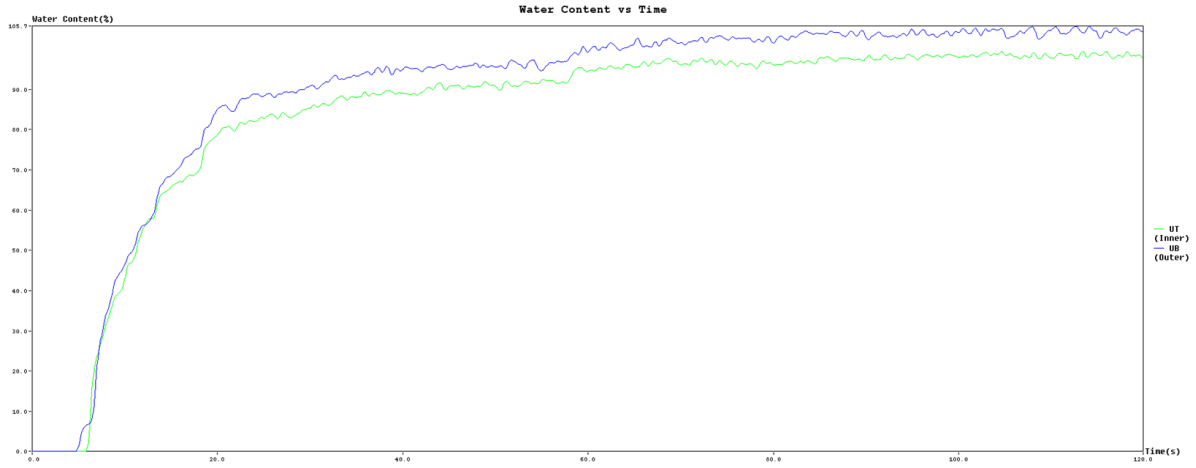

Figure4-16: Water content vs time of blue fabric (1s)

4.1.4 GATS test

The Gravimetric Absorbency Testing System (GATS) is used to measure the ability of the sample to take up liquid spontaneously in the direction perpendicular to its plane. The fabric sample was saturated with liquid and evaporation happens at the same time. Table 4.2 shows the summary of absorption properties for those three fabrics:

Table 4.2: Summary of Absorption Properties

Absorption Properties	----- Sample Identification ----- B	S	W
W_d: Dry Weight (g)	0.831	0.845	0.867
W_w: Wet Weight (g)	4.243	3.279	2.988
V: Water Displaced (g)	4.568	3.591	3.381
T: Absorption Time (min)	0.153	0.124	0.127
C: Absorbent Capacity (g)[a]	3.412	2.433	2.121
Q: Absorbency Rate (g/min)[b]	24.991	20.575	13.956
E_p: Evaporation(%)[c]	25.253	32.085	37.054

And Figure 4-17 shows the absorption behavior of those three fabrics:

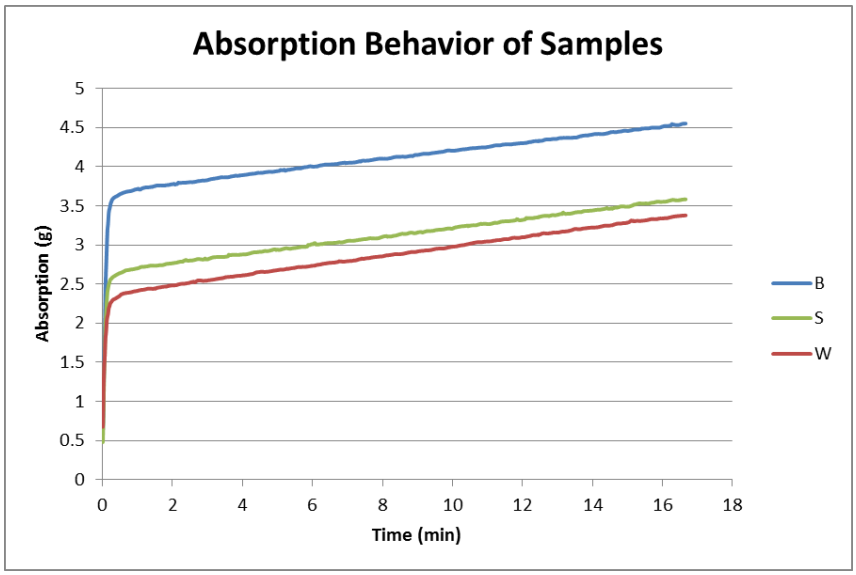

Figure 4-17: Absorption behavior of white, salmon and blue fabrics

Where we can conclude that blue fabric have the highest absorbent capacity even it has little wicking behaviors. Higher value indicates that more water has been absorbed. The reason why blue fabric can hold more water has been studied by both capillary theory and porosity of fabric.

Compared the moisture transport properties with small volume of water, when fabric is saturated with water, water not only wicks into the yarns but also covers the holes between yarns.

The porosity has been calculated following equation 2.21. The thickness of fabric has been measure by Kawabata evaluation system at 0.5cN/cm2. Table 4.3 shows that blue fabric has higher porosity than white fabric, which indicate that blue fabric can absorb more water when the fabric is totally wet.

Table 4.3: Porosity of blue and white fabrics

	Blue fabric	**White fabric**
weight	0.172g	0.187g
length	3.7cm	3.5cm
width	3.4cm	3.4cm
thickness	0.713mm	0.454mm
Fibric density	197.76 kg/m^3	336.24 kg/m^3
Fiber density	1380 kg/m^3	1380 kg/m^3
Porosity	86.10%	75.64%

We also calculated the capillary height of the perpendicular direction. If the capillary height is larger than the thickness of fabric, the holes within the loop of yarns can be totally covered with water. Based on the equation 2.18 and 2.20, $\rho gh=2\gamma LV \cos\theta/r$, where r is the radius of the hole in the loop, ρ is 1g/cm3, g is 9.8 N/Kg and γLV is 72.8 mN/m. Figure 4-18 shows the scale of the holes within the fabric. Figure 4-19 shows the contact angle of the water droplet deposited on the yarn, which equals to the θ in the equation. The radius of holes and contact angles has been measured by ImageJ.

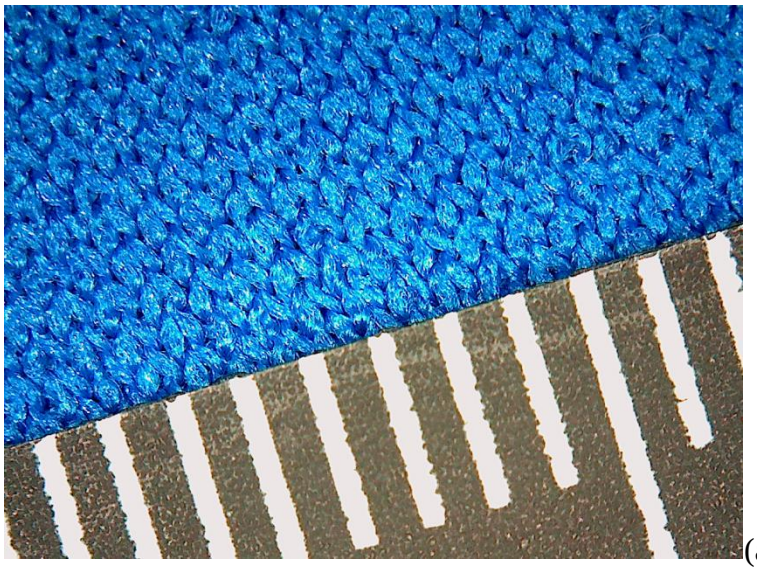
(a)

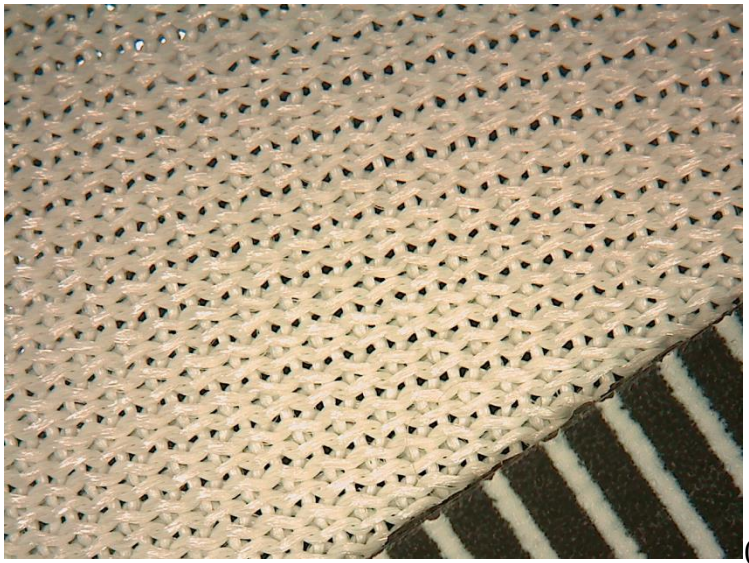
(b)

Figure 4-18: Scales of holes within the fabric. (a): Blue fabric (b): White fabric

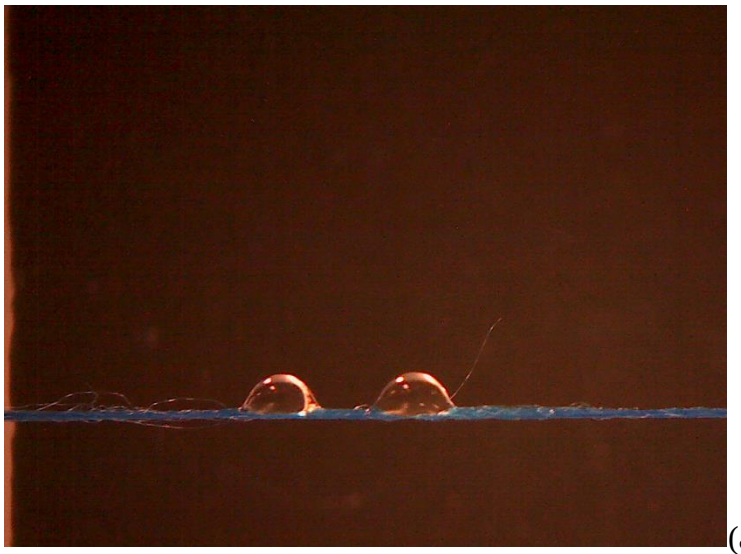

(a)

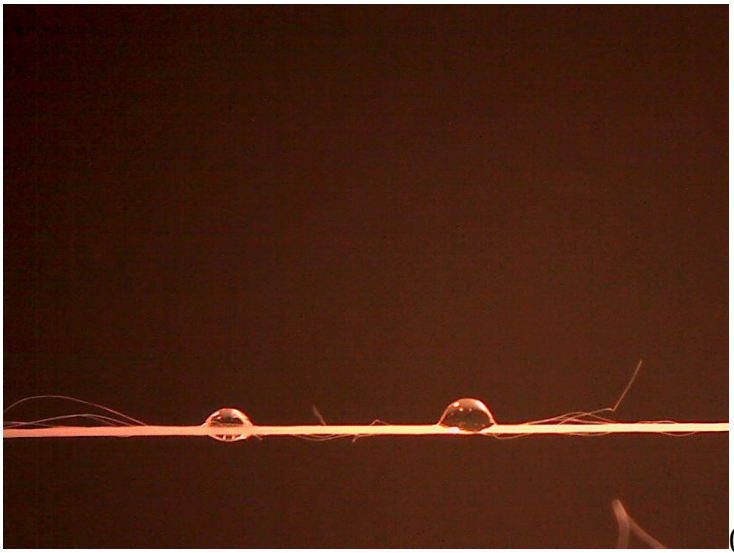

(b)

Figure 4-19: Water droplets deposited on the yarn. (a): PET yarn (b) Avra™ yarn

Table 4.4 shows the capillary height of both Blue and White fabric for the perpendicular direction:

Table 4.4 : Capillary heights of both PET and Avra™ fabrics

	Blue fabric	White fabric
Radius of hole	0.05mm	0.1mm
Contact angle	58˚	61˚
Capillary height	1.57mm	0.72mm
Thickness	0.713mm	0.454mm

Both PET and Avra™ fabric have larger capillary height compared with their thickness, which indicates that water can fill in the holes of loops when fabric is saturated with water. Also combined with porosity of both fabric, blue fabric can absorb more water as it has higher porosity and capillary height.

4.2 Create hydrophobic yarns within polyester woven and knit fabric

Fabrics with good moisture management properties can keep the body dry by keeping moisture away from the body surface in vapor and/or liquid form, and thus gives us a better comfort feeling. The base fiber properties are the main factors of the behavior of the fabric, which we have discussed in section 4.1 that with the same fabric structure, fabrics knitted with hydrophilic yarns or hydrophobic yarns show significantly different wicking phenomena. Besides the base fiber and fabric properties, the modification of fabric structure or in the finishing part can provide various features like durable water repellency or superior breathability.

Figure 4-20 shows the main problem we are facing when a human body sweats a lot during activities. When our body sweats a lot, moisture will transfer from our skin to the fabric, within the spaces between fabric surface and our skin, which causes the clingy and uncomfortable feeling. Also the moisture will fill in the spaces between fibers within the

yarns, which lead to the slow drying and give us the wet look of the textile we are wearing. In order to reduce water uptake and drying time and to modify the fabric with faster evaporation, we proposed the model as shown on the right of Figure 4-20. We modified the fabric with different hygroscopic properties for inner and outer regions of the yarns. The inner part of the yarns have been modified as hydrophobic, where moisture won't get into the spaces between fibers within the yarns, therefore it prevents the wicking behavior here. Moisture will mainly transfer from our skin to the surface of fabric through the original spaces between yarns caused by the fabric structure. With less moisture, the fabric will have faster cooling and drying properties. We also attached the surface of yarns with 'smart' thermal dynamic material, to treat the surface as hydrophilic under specific temperatures, and will be discussed in the next section.

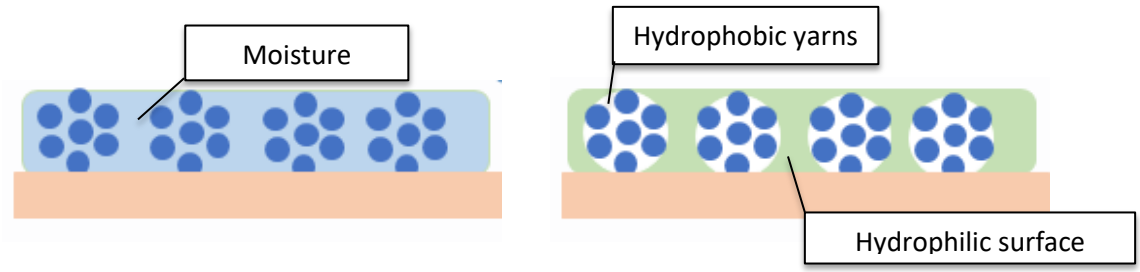

Figure 4-20: The fabric surface before(left) and after(right) modifications

The current process for this section consists of two stages with the potential of reducing this to one stage. In the first stage, a multifunctional polymer is permanently attached to the fabric for further reactions. In the second stage, a non-fluorochemical hydrophobic agent, stearyl alcohol, is bonded to the multifunctional polymer. This step renders the inside of the yarns hydrophobic, thus reducing wet pickup. These two steps may be able to be combined into one.

Two kinds of fabrics have been used in this section. The woven fabric (white) and knitted fabric (black) are both polyester fabrics. The woven fabric structure has higher

packing density, which gives us a hydrophobic surface. The knitted fabric, however, is hydrophilic, even composed with hydrophobic yarns, which because of the loose structure. We measured the contact angle and wet pick-up for both untreated fabrics. (Table 4.5)

Table 4.5: Wet pick-up and contact angles for woven and knitted fabrics.

	Wet pick-up	Contact angle at 0sec	Contact angle at 6sec
woven fabric	70%	110°	70°
knitted fabric	146%	0°	0°

The woven fabrics were chosen to be used for the preliminary experiments, with which we checked the feasibility and optimized the process. The knitted fabrics came from the commercial sportswear, which we were mainly using this fabric for the whole experiments.

4.2.1 Wetting behavior of PAA pre-treatment polyester fabric

Polyester has few reactive groups on its surface, so surface treatments are usually temporary. Yet for this application, it must be durable. To introduce reactive sites on the fiber surfaces and to chemically bond the treatments to polyester, we first react poly(acrylic acid), PAA, via a transesterification reaction between PAA and polyester. This tethers PAA to the surface and introduces many carboxylic acid groups on the surface for further reactions. A relatively small number of grafted polymer chains can potentially cover the entire surface of

the polymeric fibers using only a few graft sites. PAA is ideal for grafting because it is a highly functional polymer.

Figure 4-21 shows the mechanism of this reaction. By using dip-pad-cure process, the fabric would be covered with a thin layer of PAA with functional acid groups on the surface, which prepares it for follow-up treatments. After bonding with PAA, the surface of fabric should enhance water adsorption.

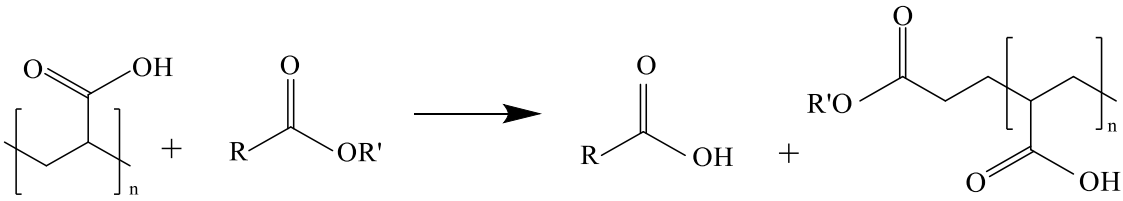

Figure 4-21: Transesterification between PAA and polyester (R')

Prior to treatment, the woven fabric had hydrophobic properties before treatment because of its structure. Its original WPU was 70% and CA was 110 °at 0s, which fell to 70 ° after 6s. In preliminary experiments, 3 and 4% PAA aqueous solution concentrations, bonding temperatures of 50, 60, 90 ℃, and cure times of 1 and 2 minutes were evaluated, conditions are summarized in Table 4.6.

Table 4.6: PAA treatment at different PAA concentrations, cure temperatures and cure times.

Concentration	Dry temperature (all for 30s)	Cure temperature	Cure time	Number of samples	Average CA after 6s	Average wet pick up
4%	50 ℃	175 ℃	1 min	2	57 °	78%
4%	60 ℃	175 ℃	1 min	3	58 °	79%
4%	90 ℃	175 ℃	1 min	2	60 °	76%
4%	50 ℃	175 ℃	2 min	3	70 °	60%
3%	50 ℃	175 ℃	1 min	2	60 °	85%
3%	50 ℃	175 ℃	2 min	3	65 °	61%

All the samples followed the 'dip-pad-cure' procedure. After curing with PAA and after the samples had been washed and dried, the fabric should show an increase of WPU and lower CA because of the new carboxyl groups on the fabric surface. The lowest CA after 6s was around 40 °, the highest wet pick-up was about 90%. After two minutes, the water droplet was spread to 0 °. The samples cured for 2 min exhibited highly variable CAs. Samples with higher concentration and longer cure time will become stiff with bad hand feeling. Based on these results, 3%PAA and 1min cure time were chosen as the best choice for PAA treatment.

Compared with the woven fabric, knitted fabric had hydrophilic properties before treatment because the loose knitted structure. Water is easy to flood into the fabric and wick into the spaces between fibers, which leads to a higher wet pick-up about 146% and longer dry time. Based on its structure, we decreased the concentration of PAA solution to 2%, and measured the contact angle and wet pick-up for this treated fabric. Because of a large number of carboxylic acid groups exposed on the surface, the PAA treated fabric has extremely small

contact angle and wet pick-up up to 176%. The content of PAA functional groups has been measured and will be discussed in a later section.

4.2.2 Wetting behavior of polyester fabric with hydrophobic yarns

In order to render the interior of the yarn hydrophobic, a long chain aliphatic alcohol, stearyl alcohol, was attached to the PAA treated fabric and infiltrated into the yarns. The same procedure 'dip-pad-cure' as above was used to graft stearyl alcohol onto and into the fabric. The ester bonds had been formed in this esterification and this step makes the interior of the yarns hydrophobic, resulting in lower wet pick up, WPU. Other long chain alcohols can be substituted for stearyl alcohol.

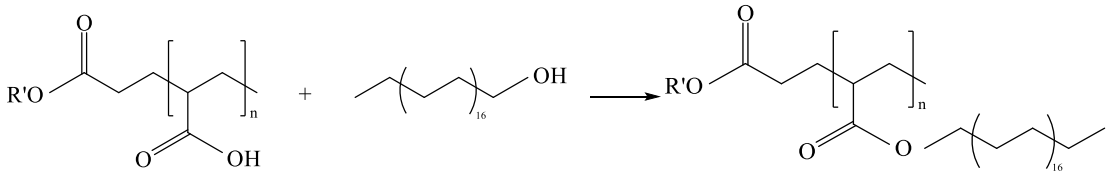

Figure 4-22: Esterification reaction of stearyl alcohol with PAA-grafted polyester fabric

It is hypothesized that after the esterification reaction, the surface and inner part of polyester fabric will be covered with one layer of ester. Both the ester and fatty carbon chains will contribute to the hydrophobic properties for the fabric. The modification process until this treatment is depicted in Figure 4-23:

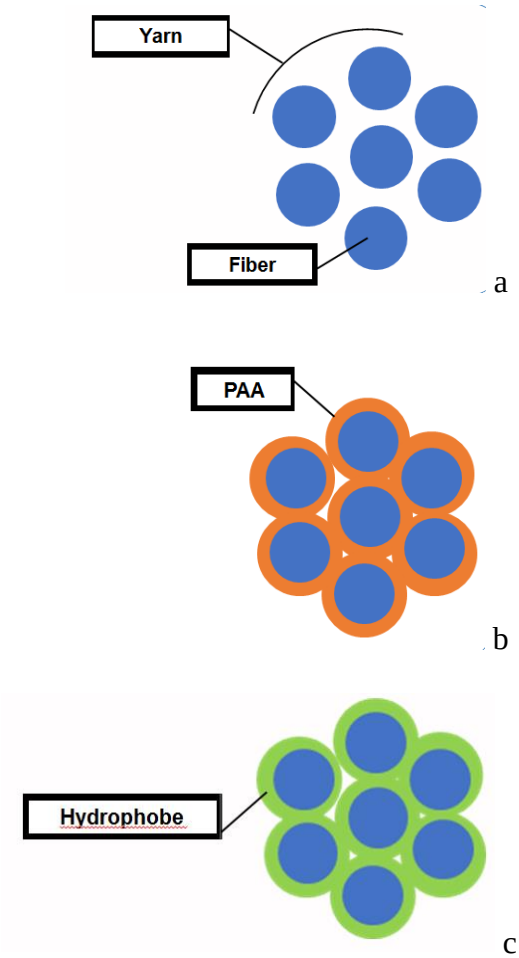

Figure 4-23: Different stages of treatment for polyester fabric with hydrophobic yarns. (a: single yarn is composed by several fibers with relative spaces; b: the surface of fibers has been covered with a layer of PAA; c: the surface of fibers has been covered with hydrophobe after the esterification reaction)

The woven fabric was chosen for preliminary experiments, its original WPU was 70% and CA was 110 °at 0s, which fell to 70 °after 6s. After it was modified with PAA, the WPU raised up to 85%. Table 4.4 shows the wetting behavior of polyester fabric treated with stearyl alcohol under different conditions. The melting temperature of stearyl alcohol is 59℃, we tried different trials of experiments under 60℃,70℃ and 80℃. According to the contact

angle and wet pick-up test results, fabrics treated with 1% of stearyl alcohol under 70 ℃ solution temperature shows both hydrophobic properties and good hand feeling. Higher concentration and temperature will cause bad hand feeling, the fabric will be rigid. Lower temperature will not allow stearyl alcohol totally melt, which is difficult for it to infiltrate into the yarns, therefore there is less chemical remained in the fabric. During the process, the fabric should be kept under the hot solution before it has been moved to padding. When temperature cools down, the stearyl alcohol will turn into solid instead of liquid, which will cause uneven treatment during curing.

Table 4.7: Stearyl Alcohol treated in aqueous solution

Alcohol %	Solution temperature	CA after 6s	Wet pick up	Comments
3%	80 ℃	100°	26%	Fabrics are rigid
2%	60 ℃	0-10 °spread quickly	65%	Fabrics are soft
2%	80 ℃	100°	25%	Fabrics are rigid
1%	70 ℃	spread slowly and large CA	50%	Fabrics are soft

Then this treatment has been moved forward to the knited fabric, with optimized concentration of stearyl alcohol solution at 1.5%. The grafting procedure was run under the combined methods, where 2%PAA and 1.5% stearyl alcohol were stirred and heated up at 70 ℃. The curing section was carried out at 175 ℃ for 2 min. Prior to treatment, this fabric showed high wet pick-up and extremely small contact angle because of its structure. After grafting with stearyl alcohol, the fabric surface has become hydrophobic and the wet pick-up

has also decreased a lot. (Figure 4-24) The photo on the left shows the wetting behavior of the original fabric, where the water droplet spread into the fabric within one seconds. However, the P-A fabric as the right photo shows can hold the droplets for a while. Here we simplify the name for this stage of treated fabric as P-A fabric.

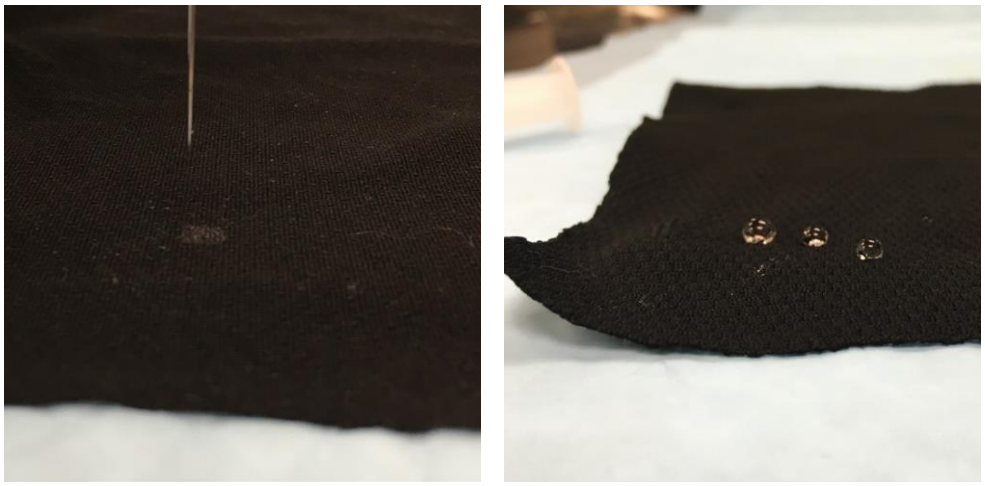

Figure 4-24: Surface wetting behavior of original fabric (left) and P-A fabric (right)

We measured the contact angle for P-A fabric as Figure 4-25 and Figure 4-26 shows:

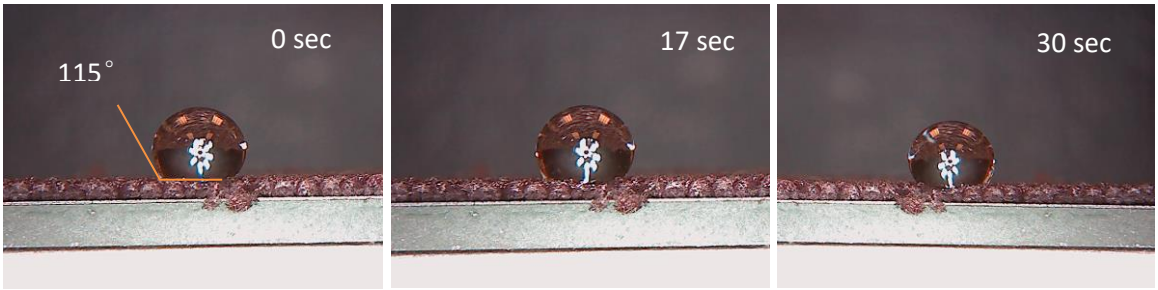

Figure 4-25: Contact angle of unwashed P-A fabric

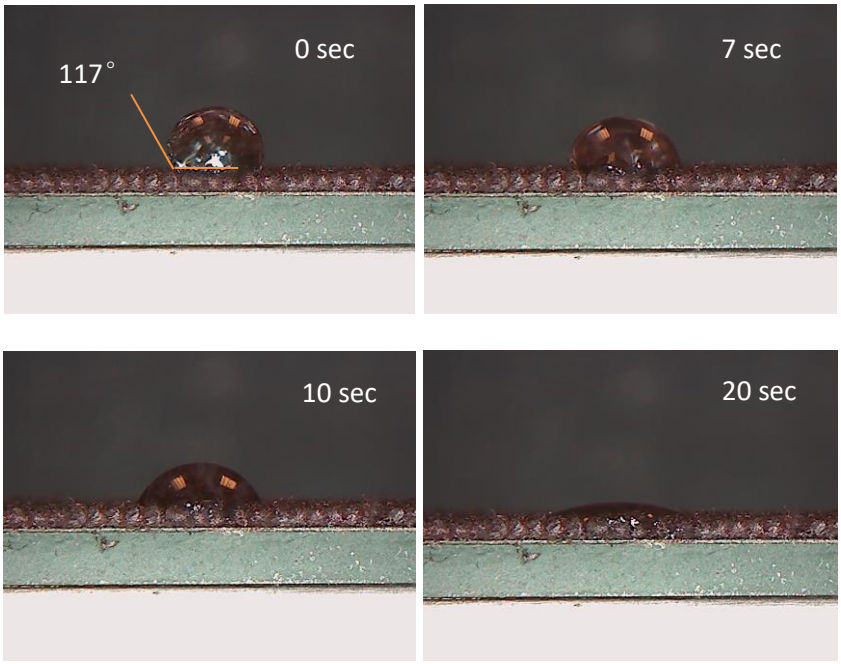

Figure 4-26: Contact angle of washed P-A fabric

The unwashed fabric retained excessive chemical on the surface, which can hold the droplet for long time, the contact angle stayed as 115 °. The washed fabric has hydrophobic surface properties, with large contact angle around 117 °at the beginning, and then it spread into the spaces between yarns gradually, and disappears after 25 seconds. Compared with the original fabric surface, the P-A fabric has been modified with hydrophobic surface behavior. The wetting behavior on the surface, or the degree of hydrophobic property would be expected as various, depending on the content of PAA acid groups and stearyl alcohol hydrophobic side chains on the fabric surface, which has been measured and discussed in the next section. Wet pick-up is another important factor to describe the moisture management behavior of fabric. According to the theory and hypothesis, as for the inner part of yarns have been modified as hydrophobic, where water cannot go through into the spaces between fibers, therefore the fabric will pick up less water. Here we measured the wet pick-up for each stage of treated fabric:

Table 4.8: Wet pick-up tests

	Wet pick-up
Untreated knitted fabric	146%
PAA treated fabric	176%
P-A fabric	80%

The untreated knitted fabric has high wet pick-up around 146% because of its loose structure, where water could wick into fabric easily. The PAA treated fabric has large amount of carboxylic acid groups on the surface that contributed to the water absorption and led to a higher wet pick-up at around 176%. The P-A fabric has significantly lower water content, around 80%, which decreases more than 60% compared with untreated fabric. A thin layer of ester formed through esterification has covered the spaces between fibers, where the inner part of yarns have been treated as hydrophobic. Water just transports through spaces between yarns and less wicking happens within the yarns. Therefore the fabric has less wet pick-up and should dry faster.

In order to determine whether the treated fabric will dry quicker than the original fabric, a drying rate test was performed following AATCC 201, Table 4.9. These results show that, in terms of volume, the drying rate for the treated and untreated fabrics were similar; the treated fabric may dry slightly slower than the untreated one. However, considering that the amount of water picked up by the treated fabric is about 55% of that picked up by the untreated fabric, the time required to dry the treated fabric would be half of the time required for the untreated fabric.

Table 4.9: Drying rate

Sample ID	Drying Rate mL/h
Treated -1	1.35
-2	1.43
Avg.	**1.39**
Untreated -1	1.60
-2	1.41
Avg.	**1.51**

4.2.3 PAA content after treatment

The content of PAA for each stage of the knitted fabric has been quantified by a colorimetric method using Toluidine Blue O (TBO), which was based on the number of carboxyl groups grafted onto the fabric. The untreated fabric, PAA treated fabric and after stearyl alcohol grafted fabric have all been tested separately. The content of PAA for each stage could show the density of grafted PAA at the beginning and how much PAA has had connection with stearyl alcohol directly, as it is important to determine the hydrophilicity for treated fabrics later.

The original fabrics are used for control sample which have no PAA on the fiber surface. But because the fabric will take up dye via adsorption under the conditions, the control sample should also measure the amount of dye up take as well. The absorbance of the control samples were subtracted from the grafted sliver to obtain the absorbance due to the attached PAA. The polymer graft concentration was calculated from the standard curve. (Figure 4-27)

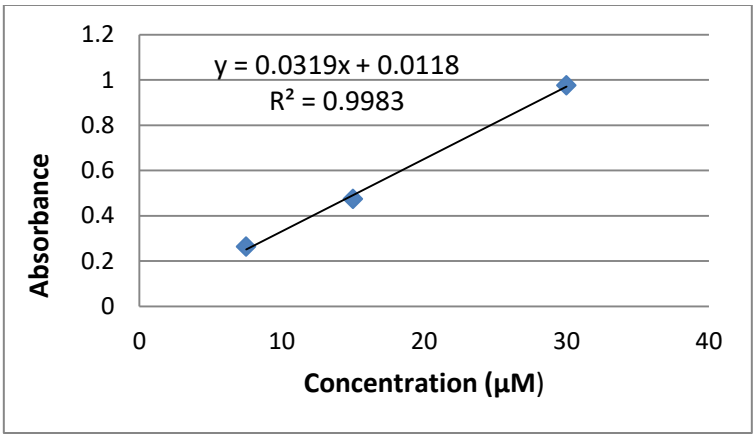

Figure 4-27: Toluidine blue O standard curve to determine poly(acrylic acid) content

Using the method introduced above, amounts of carboxyl groups on the polyester fabric surface were measured as shown in Table 4.10. The TBO amount attached on the polyester fabric was found to lie in the 95% confidence interval of 1.55±0.27 μmol per gram of fabric.

Table 4.10: TBO content on polyester fabric surface

Polyester fabric	Absorbance	TBO Content (μmol/g)
1	0.061	1.542
2	0.065	1.668
3	0.058	1.448
Average		1.552
Standard Deviation		0.11
Margin of Error		0.27

The amounts of carboxyl groups on the polyester-PAA fabric surface were measured shown in Table 4.11, where the TBO amount attached on the polyester-PAA fabric was found to lie in the 95% confidence interval of 9.68±0.34 μmol per gram of fabric.

Table 4.11: TBO content on polyester-PAA fabric surface

Polyester-PAA fabric	Absorbance	TBO Content (μmol/g)
1	0.321	9.693
2	0.316	9.536
3	0.325	9.818
Average		9.682
Standard Deviation		0.14
Margin of Error		0.34

Also, the amounts of carboxyl groups on the polyester-PAA-stearyl alcohol fabric(P-A fabric) surface were measured shown in Table 4.12, where the TBO amount attached on the polyester-PAA-stearyl alcohol fabric was found to lie in the 95% confidence interval of 7.09±0.7 μmol per gram of fabric.

Table 4.12: TBO content on polyester-PAA-stearyl alcohol fabric surface

P-A fabric	Absorbance	TBO Content (μmol/g)
1	0.230	6.840
2	0.248	7.404
3	0.236	7.028
Average		7.09
Standard Deviation		0.28
Margin of Error		0.7

The content of carboxylic acids from PAA attached to fabric surface versus TBO is believed to be 1:1. [38]After subtracting the value of untreated fabric, the content of –COOH in PAA grafted fabric is around 8.128 μmol/(g fabric), and the content of –COOH in PAA-stearyl alcohol grafted fabric is around 5.538 μmol/(g fabric). Thus, there are around 31.86% of acid groups has been connected for reaction.

Even with 31.86% covered of ester, the long carbon chains from stearyl alcohol will precipitate on the top of PAA grafted surface, which will prevent the contact between the rest of acid groups and moisture. This can be explained for the contact angle measured in section 4.2.2, with excessive chemical, the surface has become totally hydrophobic; after washing, the contact angle is large at the beginning but water droplet can still spread along the fabric slowly which is caused by the remaining acid groups on the surface.

4.3 Attach ‘smart’ wetting technology on the fabric surface

After the modification of creating hydrophobic yarns, moisture could not get into the inner part of the yarns, which reduced wicking between fibers. Based on this, a new dynamic moisture management strategy and system have been developed and applied to knitted sportswear fabric, which provided faster drying at elevated temperature. At room temperature, the surface of treated fabric is hydrophilic, but the inner part of yarns in hydrophobic. This is expected to reduce dry time and prevent the “wet look”. As the skin temperature rises, the fabric surface becomes hydrophobic thus decreasing wetting and wicking within the fabric, but allowing faster moisture transport from skin to out layer of fabric through interspace of knit structure at elevated temperature. However, the fabric could maintain its low moisture pickup, which should reduce the “wet look” and the drying time. Figure 4-28 shows the modification for this stage:

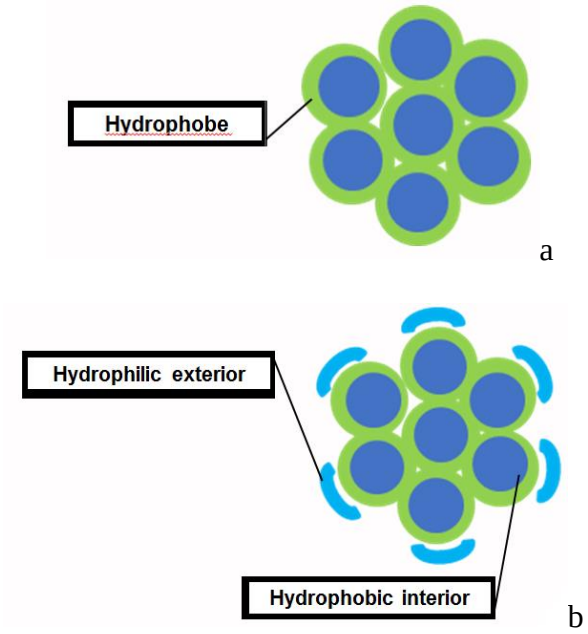

Figure 4-28: Surface treatment with ‘smart’ wetting technology

Here, a dynamic moisture managing permanent treatment is attached to the yarn surfaces, thus creating a material that should be hydrophilic at room temperature and hydrophobic at temperatures above 32℃. To impart dynamic characteristics, a temperature-responsive hydrogel is added to the surface. The hydrogel we used is PNIPAM (poly(N-isopropylacrylamide)), which changes its water solubility below and above the LCST (lower critical solution temperature). (Figure 4-29)

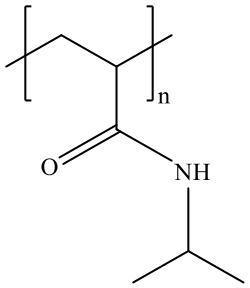

Figure 4-29: Chemical structure of poly(N-isopropylacrylamide), PNIPAM

PNIPAM cannot be grafted directly to PAA, so N-isopropylacrylamide was copolymerized with 2-aminoethyl methacrylate, AEMA (Figure 4-30). This introduced amino groups into PNIPAM that can graft to PAA. Figure 4-31 shows the copolymerization of NIPAM and AEMA.

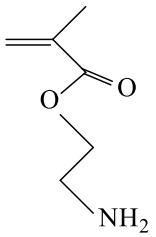

Figure 4-30: Chemical structure of 2-aminoethyl methacrylate, AEMA

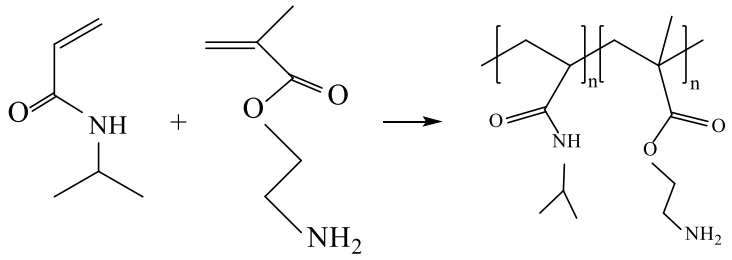

Figure 4-31: Copolymerization of NIPAM and AEMA

Finally, P(NIPAM-co-AEMA) could be bonded to the surface of modified PET fabric through pad and cure process. (Figure 4-32) Since P(NIPAM-co-AEMA) is water soluble and water is prevented from entering the yarns within the fabric, only the surface of the yarns were modified with P(NIPAM-co-AEMA).

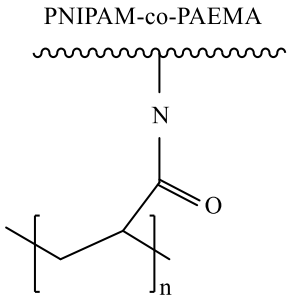

Figure 4-32: PNIPAM-co-PAEMA grafted to PAA-modified polyester

The wetting behavior of treated fabric has been evaluated for both room temperature and elevated temperature, in order to simulate the condition when human temperature increases during activities.

4.3.1 Synthesis of the moisture management copolymer

PNIPAM is a temperature-responsive hydrogel that has different solubility below and above its LCST. When it is bonded to the surface, the fabric should change its behavior when contacting with water at temperatures above and below the LCST. After polymerizing

P(NIPAN-co-AEMA), the DSC test was run to ensure this new polymer exhibited the same LCST and the original PNIPAM. The results are shown in Figure 4-33. The DSC test results show that the LCST was 32.9 ℃ on heating and 29.9 ℃ on cooling, which is similar to the LCST for PNIPAM.[74]

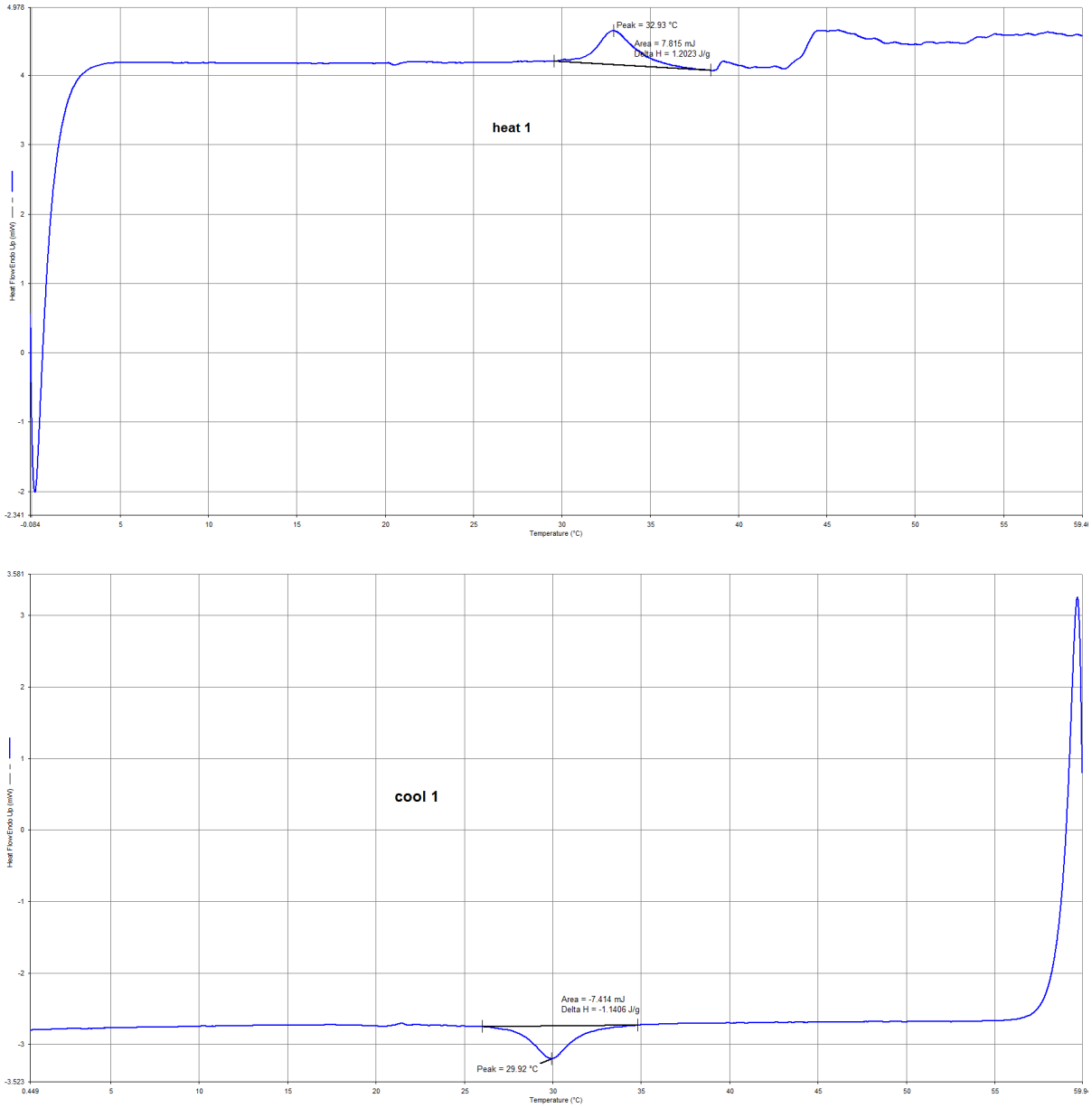

Figure 4-33: DSC scans for both heating (top) and cooling (bottom) figures

2-aminoethyl methacrylate, (AEMA), is used for providing functional groups to connect with PAA during curing, and there is only a small amount of AEMA for the copolymer, the LCST for the copolymer is still dominant by PNIPAM. Figure 4-34 shows the copolymer aqueous solution at different temperature. With higher temperature, the copolymer solution became cloudy, where phase separation happens.

Figure 4-34: P(NIPAN-co-AEMA) aqueous solution at elevated(left) and room(right) temperature

4.3.2 Wetting behavior of ‘smart’ fabric

The ‘smart’ fabric should present dynamic moisture management behavior under different temperatures. According to the theory, at room temperature which is below LCST (32℃), PNIPAM should be hydrophilic that could attract and hold water. Above LCST, PNIPAM chains independently phase separate and shrink, which shows hydrophobic properties. The mechanism of wetting behavior for this ‘smart’ fabric would be complicated, as it contributed by the content of PAA acid groups, stearyl alcohol long chains and also the thermal sensitive polymer PNIPAM. We measured the wet-pick up and contact angle for all

stages of treated fabrics both under room temperature (20℃) and elevated temperature (40℃).

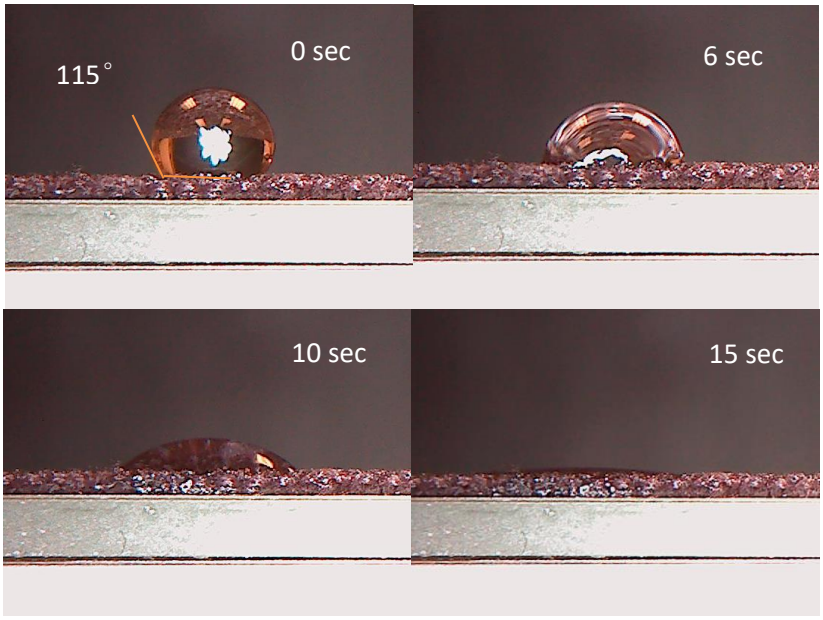

Figure 4-35: Contact angle of unwashed PNIPAM treated fabric at 20℃

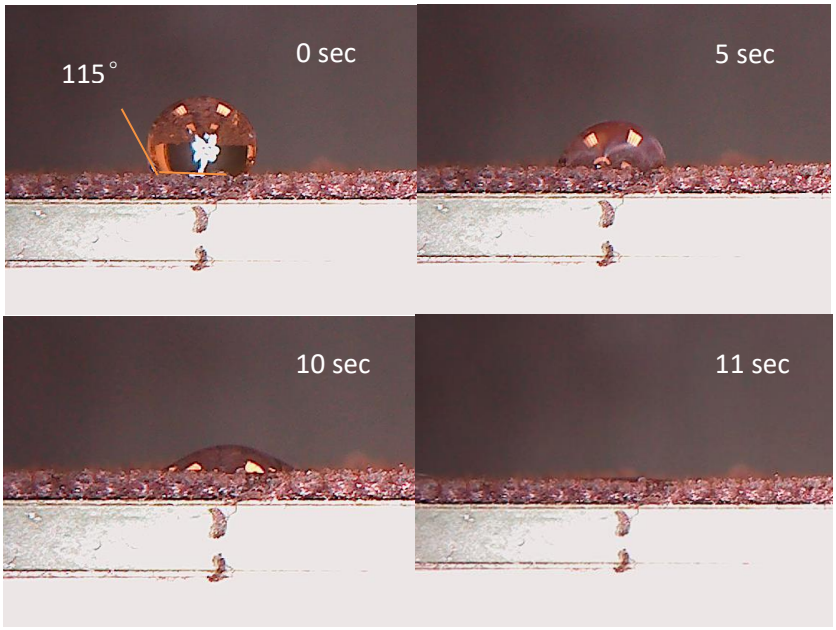

Figure 4-36: Contact angle of washed PNIPAM treated fabric at 20℃

Figure 4-35 and 4-36 shows the contact angle of PNIPAM treated fabric for both unwashed after grafted with stearyl alcohol and washed one. The surface is hydrophobic at beginning, and then water spread into the fabric after 15 seconds. The washed fabric has shorter spreading time because of excessive chemical on the surface has been washed off. Compared with P-A fabric in Figure 4-25, PNIPAM has some contribution to the hydrophilic properties of surface, but not significant. The wet pick-up is similar as P-A fabric around 80% because the inner part of fabric has been treated as hydrophobic. When temperature rose up, the surface is highly hydrophilic that liquid will wick into the fabric within one second. This phenomenon conflicts with theory, that the surface should be hydrophobic at elevated temperature. So we compared with the wetting behavior of PAA-PNIPAM treated fabric. The contact angle shows from Figure 4-37 indicate that fabric surface just coated with PAA and PNIPAM is hydrophilic, the crosslinked polymer may cover the spaces between yarns but liquid will soon wick into the fabric. But at elevated temperature 40℃, liquid will wick into the fabric even faster, which also conflicts with theory. Therefore we concluded that,

PNIPAM has little contribution for the treated fabric, the surface property is mainly result from the acid groups from PAA. When temperature goes up, PNIPAM chains shrink where more PAA acid groups appear on the surface leads to the faster wicking behavior.

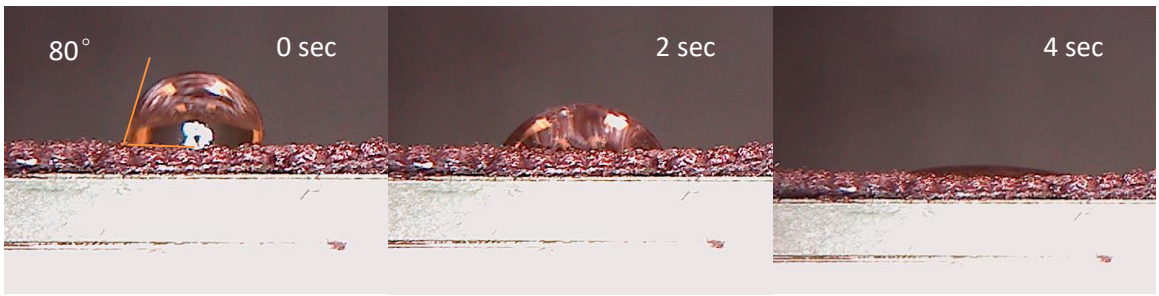

Figure 4-37: Contact angle of PAA-PNIPAM treated fabric at 20℃

We also studied the wetting behavior for all different treated fabrics under both room and elevated temperature as Table 4.13 shows:

Table 4.13: Wet pick-up and contact angle for all stages fabrics under different temperature

	Wet pick-up (20℃)	**Wet pick-up (40℃)**	**Contact angle (20℃)**	**Contact angle (40℃)**
Untreated fabric	146%	142%	0°	0°
PAA treated	176%	161%	0°	0°
P-A fabric	80%	117%	115°	0°
P-A-PNIPAM fabric	80%	115%	115°	0°

At elevated temperature, all stages of fabrics have hydrophilic surface where liquid spread into fabric quickly even with P-A fabric. As temperature goes up, part of the precipitated stearyl alcohol starts to become soft, the motion of polymer chains allow more PAA acid groups to be exposed to the liquid and increased the hydrophilic properties of the surface a lot. The wet pick-up of P-A fabric at 40℃ has increased to 117% compared with 80% at room temperature, but most inner part of the fabric is still hydrophobic, compared with the wet pick-up of untreated fabric of 142%. The P-A fabric performs different moisture management properties under different temperature, which is benefit to be used for faster drying sportswear. At room temperature, the fabric is hydrophobic for the inner part, which allows less water content. When temperature rises, the surface of fabric become hydrophilic,

which provides lager surface area for moisture evaporation. The dynamic moisture management properties can be controlled by the content of PAA and stearyl alcohol, and PNIPAM has little contribution for the treated fabric here.

5. CONCLUSION

5.1 Wicking behavior of different fabrics

Three different fabrics provided by Eastman with the same knitted structure have been studied on their moisture transport behavior with 1 μL of water. The moisture transport behaviors are various which caused by the morphology difference of the yarns. The wetting behaviors of these three fabrics have been investigated by image analysis, drying time measurement and standard moisture property measurement by using moisture management tester (MMT). As for image analysis results, the wetting area on white fabric presents as round shape, however, on the salmon fabric it presents as long strip. Compared with these two fabrics, there is little wicking within blue fabric, whose wetting area doesn't change a lot from when droplet deposited on the surface. This is because that polyester yarn is hydrophobic, which has less moisture transport property rather than hydrophilic yarns. The wicking distance measurement also convinced this phenomenon, where water mainly wicked into the hydrophilic yarns. For the drying time of these three fabrics, white fabric has shortest drying and followed by salmon fabric, blue fabric dries much slower than the others. Three fabrics have also been tested with MMT by running different pump volumes. Fabrics showed different One-way Transport Capability and water content tendency between larger water volume (12 μL) and small volume (1 μL).

5.2 Wetting behavior of polyester fabric with hydrophobic yarns

Knitted fabric has been modified with different hydrophilic properties for inner and outer regions of the yarns. The inner part of the yarns has been modified as hydrophobic, where the wicking behavior has been prevented. The surface of fabric was first been treated with PAA, and then a non-fluorochemical hydrophobic agent, stearyl alcohol, has been

bonded to the multifunctional surface, where the esterification reaction happened. The treated fabric surface was hydrophobic with large contact angle and less than 60% water pick-up compared with untreated fabric. The content of PAA for both PAA treated fabric and PAA-stearyl alcohol treated fabrics have been measured. About 32% PAA acid groups have been used after the esterification.

5.3 Wetting behavior of 'smart' fabric

The copolymer, P(NIPAM-co-AEMA) has been synthesized and grafted on the surface of P-A fabric successfully. The contact angle and wet pick-up have been measured under two different temperature, 20℃ and 40℃. The result showed that the thermal dynamic copolymer had little contribution to adjust the moisture management properties of the fabric. However, the surface of P-A fabric turned to be hydrophilic at elevated temperature, where the stearyl alcohol started to melt and surface property was mainly result from the acid groups from PAA. The P-A fabric showed different surface property under room and elevated temperature.

6. FUTURE WORK

1. The wetting and wicking behavior on the fabric surface with different morphology of fibers has been studied. Currently the comparison is between Avra™ fabric and PET fabric based on the same knitted structure. For further study, the wicking behavior of single yarn or two parallel yarns can be observed. Also, a model for the drying time of fabric with 1μL of water can be constructed.

2. The surface modification of sports fabric can be optimized on the content of functional groups or the concentration of solution we used. For this work, about 30% acid groups form PAA on the surface has been reacted with stearyl alcohol, as the surface property changed at elevated temperature. For the further study, the surface wetting property can be adjusted with various content of PAA and stearyl alcohol.

3. The dynamic thermal properties of PNIPAM can be modulated with different techniques. We could try different methods for shifting the LCST of PNIPAM, and apply this polymer on the fabric surface based on the optimization proposed above.

REFERENCES

1. About Sports Textiles. Available at: http://www.technicaltextile.net/sports-textiles/. (Accessed: 1st January 2016)

2. Sports Textile/Sporttech | Properties of Sports Textile | Application/Uses of Sports Textile. Available at: http://textilelearner.blogspot.in/2012/03/sports-textilesporttech-properties-of.html. (Accessed: 24th December 2012)

3. Uttam, D., Zail, G. & Campus, S. Active sportswear fabrics. *Int. Journel IT, Eng. Appl. Sci. Res.* 2, 34–40 (2013).

4. Sanjay Gupta. Smart Textiles: Their Production and Marketing Strategies : Proceedings. in 249 (National Institute of Fashion Technology, 2000).

5. Sule, A. D., R. K. Sarkar, M. K. B. Development of sportswear for Indian conditions. in 123–129 (Manmade Textiles in India, 2004).

6. Marchand, A., Weijs, J. H., Snoeijer, J. H. & Andreotti, B. Why is surface tension a force parallel to the interface? *Am. J. Phys.* 79, 999 (2011).

7. Adamson, A. W. & Gast, A. P. Physical Chemistry of Surfaces. (1967).

8. Fujii, H. & Nakae, H. Effect of gravity on contact angle. *Philos. Mag. A* 72, 1505–1512 (1995).

9. Diez, J. a., Gratton, R., Thomas, L. P. & Marino, B. Laplace pressure driven drop spreading. *Phys. Fluids* 6, 24–33 (1994).

10. Schrader, M. E. Young-Dupre Revisited. *Langmuir* 11, 3585–3589 (1995).

11. Lee, H. J. & Michielsen, S. Lotus effect: superhydrophobicity. *J. Text. Inst.* 97, 455–462 (2006).

12. Schrader, M. E. Young- Dupre Revisited. *Langmuir* 11, 3585–3589 (1995).

13. Fowkes, F. M. ADDITIVITY OF INTERMOLECULAR FORCES AT INTERFACES. I. DETERMINATION OF THE CONTRIBUTION TO SURFACE AND INTERFACIAL TENSIONS OF DISPERSION FORCES IN VARIOUS LIQUIDS [1]. *J. Phys. Chem.* 67, 2538–2541 (1963).

14. Cassie, B. D., Cassie, A. B. D. & Baxter, S. Wettability Of porous surfaces,. *Trans. Faraday Soc.* 40, 546–551 (1944).

15. Wenzel, R. N. Resistance of Solid Surfaces. *Ind. Eng. Chem.* 28, 988–994 (1936).

16. Marmur, A. The lotus effect: Superhydrophobicity and metastability. *Langmuir* 20, 3517–3519 (2004).

17. Kissa, E. Wetting and Wicking. *Text. Res. J.* 66, 660–668 (1996).

18. WEI, Q. *Surface Modification of Textiles*. *Woodhead Publishers* 1, (2009).

19. Feng, L. *et al.* A super-hydrophobic and super-oleophilic coating mesh film for the separation of oil and water. *Angew. Chemie - Int. Ed.* 43, 2012–2014 (2004).

20. Uyama, Y., Kato, K. & Ikada, Y. Surface Modification of Polymers by Grafting. *Grafting/Characterization Tech. Model.* 137, 1–39 (1998).

21. Tobiesen, F. A. & Michielsen, S. Method for grafting poly(acrylic acid) onto nylon 6,6 using amine end groups on nylon surface. *J. Polym. Sci. Part A Polym. Chem.* 40, 719–728 (2002).

22. Stamm, M. *Polymer Surfaces and Interfaces*. (2008). doi:10.1007/978-3-540-73865-7

23. Cross section shapes of fibers. Available at: https://gemsw.wordpress.com/2015/03/01/textile-fibres/. (Accessed: 1st January 2017)

24. Gupta, B., Saxena, S., Grover, N. & Ray, A. R. Technical Textile Yarns. Technical Textile Yarns (2010). doi:10.1533/9781845699475.2.452

25. LIM, J. Creation of Woven Structures Impacting Self-cleaning Superoleophobicity. (North Carolina State University, 2014).

26. Sinclair, R. Textiles and Fashion: Materials, Design and Technology. Textiles and Fashion: Materials, Design and Technology (2014). doi:10.1016/C2013-0-17410-7

27. Henze, M., Mädge, D., Prucker, O. & Rühe, J. 'Grafting through': Mechanistic aspects of radical polymerization reactions with surface-attached monomers. Macromolecules 47, 2929–2937 (2014).

28. Datta, P. & Genzer, J. 'Grafting Through' polymerization involving surface-bound monomers. J. Polym. Sci. Part A Polym. Chem. 54, 263–274 (2016).

29. Datta, P. & Genzer, J. Computer simulation of template polymerization using a controlled reaction scheme. Macromolecules 46, 2474–2484 (2013).

30. Fallis, A. . Plasma Technologies for Textiles 2007. Journal of Chemical Information and Modeling 53, (2013).

31. Favia, P. & d'Agostino, R. Plasma treatments and plasma deposition of polymers for biomedical applications. Surf. Coatings Technol. 98, 1102–1106 (1998).

32. Kato, K., Uchida, E., Kang, E. T., Uyama, Y. & Ikada, Y. Polymer surface with graft chains. Prog. Polym. Sci. 28, 209–259 (2003).

33. Spinning, T. Gamma-Ray-Induced Graft Copolymerization of Styrene onto cellulose and some chemical properties of the grafted polymer. 51, 359–372 (1961).

34. Dargaville, T. R., George, G. A., Hill, D. J. T. & Whittaker, A. K. High energy radiation grafting of fluoropolymers. Prog. Polym. Sci. 28, 1355–1376 (2003).

35. Yagci, Y., Jockusch, S. & Turro, N. J. Photoinitiated polymerization: Advances, challenges, and opportunities. Macromolecules 43, 6245–6260 (2010).

36. Buchen, J. Modification of Polyester Fibers by Grafting with Poly (acrylic acid). J. Appl. Polym. Sci. 967–977 (1996).

37. Sherrill, J., Michielsen, S. & Stojiljkovic, I. Grafting of light-activated antimicrobial materials to nylon films. J. Polym. Sci. Part A Polym. Chem. 41, 41–47 (2002).

38. Iyer, S. P. Immobilizing Laccase from Pleurotus ostreatus on Cotton Sliver for the Treatment of Textile Dye Effluents. (North Carolina State University, 2014).

39. Crespy, D. & Rossi, R. M. Temperature-responsive polymers with LCST in the physiological range and their applications in textiles. Polymer International 56, 1461–1468 (2007).

40. Jain, K., Vedarajan, R., Watanabe, M., Ishikiriyama, M. & Matsumi, N. Tunable LCST behavior of poly(N-isopropylacrylamide/ionic liquid) copolymers. Polym. Chem. 6, 6819–6825 (2015).

41. Kohno, Y. et al. Thermoresponsive polyelectrolytes derived from ionic liquids. Polym. Chem. 6, 2163–2178 (2015).

42. Flory, P. J. & Krigbaum, W. R. Thermodynamics of High Polymer Solutions. Annu. Rev. Phys. Chem. 2, 383–402 (1951).

43. Huggins, M. L. Solutions of Long Chain Compounds. J. Chem. Phys. 9, 440 (1941).

44. Young, Robert J., P. A. L. Introduction to polymers. (2011).

45. Lower critical solution temperature. Available at: https://www.wikiwand.com/en/Lower_critical_solution_temperature. (Accessed: 1st January 2016)

46. Patterson, D. Free Volume and Polymer Solubility. A Qualitative View. *Macromolecules* 2, 672–677 (1969).

47. Allen, G. & Baker, C. H. Lower critical solution phenomena in polymer-solvent systems . *Polymer (Guildf).* 6, 181–191 (1965).

48. Ward, M. A. & Georgiou, T. K. Thermoresponsive polymers for biomedical applications. *Polymers (Basel).* 3, 1215–1242 (2011).

49. Shimizu, K., Fujita, H. & Nagamori, E. Oxygen plasma-treated thermoresponsive polymer surfaces for cell sheet engineering. *Biotechnol. Bioeng.* 106, 303–310 (2010).

50. Doorty, K. B. *et al.* Poly(N-isopropylacrylamide) co-polymer films as potential vehicles for delivery of an antimitotic agent to vascular smooth muscle cells. *Cardiovasc. Pathol.* 12, 105–110 (2003).

51. Stile, R. A. & Healy, K. E. Thermo-responsive peptide-modified hydrogels for tissue regeneration. *Biomacromolecules* 2, 185–194 (2001).

52. Hacker, M. C., Klouda, L., Ma, B. B., Kretlow, J. D. & Mikos, A. G. Synthesis and characterization of injectable, thermally and chemically gelable, amphiphilic poly(N-isopropylacrylamide)-based macromers. *Biomacromolecules* 9, 1558–1570 (2008).

53. Vihola, H., Laukkanen, A., Tenhu, H. & Hirvonen, J. Drug release characteristics of physically cross-linked thermosensitive poly(N-vinylcaprolactam) hydrogel particles. *J. Pharm. Sci.* 97, 4783–4793 (2008).

54. Pasparakis, G. & Vamvakaki, M. Multiresponsive polymers: nano-sized assemblies, stimuli-sensitive gels and smart surfaces. *Polym. Chem.* 2, 1234 (2011).

55. Patrickios, C. S. & Georgiou, T. K. Covalent amphiphilic polymer networks. *Current Opinion in Colloid and Interface Science* 8, 76–85 (2003).

56. Meng, F., Zhong, Z. & Feijen, J. Stimuli-responsive polymersomes for programmed drug delivery. *Biomacromolecules* 10, 197–209 (2009).

57. Sawamoto, M. Modern cationic vinyl polymerization. *Progress in Polymer Science* 16, 111–172 (1991).

58. Plunkett, K. N., Zhu, X., Moore, J. S. & Leckband, D. E. PNIPAM chain collapse depends on the molecular weight and grafting density. *Langmuir* 22, 4259–4266 (2006).

59. Fundueanu, G., Constantin, M. & Ascenzi, P. Fast-responsive porous thermoresponsive microspheres for controlled delivery of macromolecules. *Int. J. Pharm.* 379, 9–17 (2009).

60. Stayton, P. S. *et al.* Control of protein-ligand recognition using a stimuli-responsive polymer. *Nature* 378, 472–474 (1995).

61. Winnik, F. M., Ottaviani, M. F., Bossmann, S. H., Garcia-Garibay, M. & Turro, N. J. Consolvency of Poly(N-isopropylacrylamide) in Mixed Water-Methanol Solutions: A Look at Spin-Labeled Polymers. *Macromolecules* 25, 6007–6017 (1992).

62. Maeda, Y. & Yamabe, M. A unique phase behavior of random copolymer of N-isopropylacrylamide and N,N-diethylacrylamide in water. *Polymer (Guildf).* 50, 519–523 (2009).

63. Van Durme, K., Rahier, H. & Van Mele, B. Influence of additives on the thermoresponsive behavior of polymers in aqueous solution. *Macromolecules* 38, 10155–10163 (2005).

64. Schild, H. G. & Tirrell, D. A. Interaction of Poly(N-isopropylacrylamide) with Sodium n-Alkyl Sulfates in Aqueous Solution. *Langmuir* 7, 665–671 (1991).

65. McPhee, W., Tam, K. C. & Pelton, R. Poly(N-isopropylacrylamide) Latices Prepared with Sodium Dodecyl Sulfate. *J. Colloid Interface Sci.* 156, 24–30 (1993).

66. Karjalainen, E., Chenna, N., Laurinmäki, P., Butcher, S. J. & Tenhu, H. Diblock copolymers consisting of a polymerized ionic liquid and poly(N-isopropylacrylamide). Effects of PNIPAM block length and counter ion on self-assembling and thermal properties. *Polym. Chem.* 4, 1014–1024 (2013).

67. Mi Kyong Yoo, Yong Kiel Sung, Chong, S. C. & Young, M. L. Effect of polymer complex formation on the cloud-point of poly(N-isopropyl acrylamide) (PNIPAAm) in the poly(NIPAAm-co-acrylic acid): polyelectrolyte complex between poly(acrylic acid) and poly(allylamine). *Polymer (Guildf).* 38, 2759–2765 (1997).

68. Oosawa, F. *Polyelectrolytes*. *Polyelectrolytes* (1971).

69. Chen, G. & Hoffman, A. S. graft copolymers of N-isopropylacrylamide and acrylic acid. *Macromol. Rapid Commun.* 182, 175–182 (1995).

70. Chen, G. & Hoffman, A. S. Graft copolymers that exhibit temperature-induced phase transitions over a wide range of pH. *Nature* 373, 49–52 (1995).

71. Chen, H. & Fang, Y. Synthesis and characterization of temperature and pH responsive Poly (N-isopropylacrylamide) copolymer. in *AIChE Annual Meeting* (2013).

72. Jones, M. S. Effect of pH on the lower critical solution temperatures of random copolymers of N -isopropylacrylamide and acrylic acid. *Eur. Polym. J.* 35, 795–801 (1999).

73. Konopka, A., Kim, H. S. & Pourdeyhimi, B. In-Plane Liquid Distribution of Nonwoven Fabrics : Part I , Experimental Observations. *Int. J. Nonwovens,* 11(4), 22–27 (2002).

74. Hofmann, C. & Schönhoff, M. Do additives shift the LCST of poly (N-isopropylacrylamide) by solvent quality changes or by direct interactions? *Colloid Polym. Sci.* 287, 1369–1376 (2009).

APPENDIX

APPENDIX A

The appendix A is referred to the wicking distance of both white and salmon fabric at certain time points, page 76. Both wicking distances for wale direction and course direction have been measured.

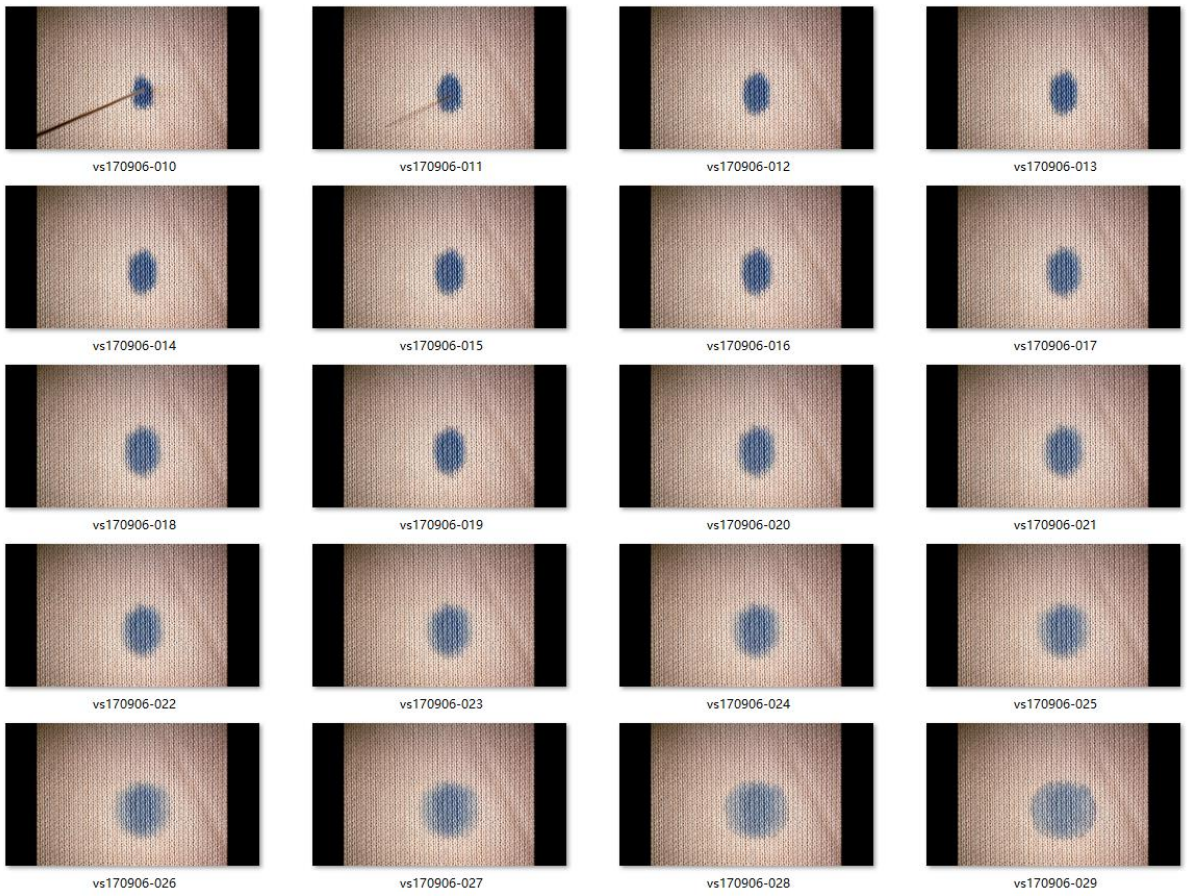

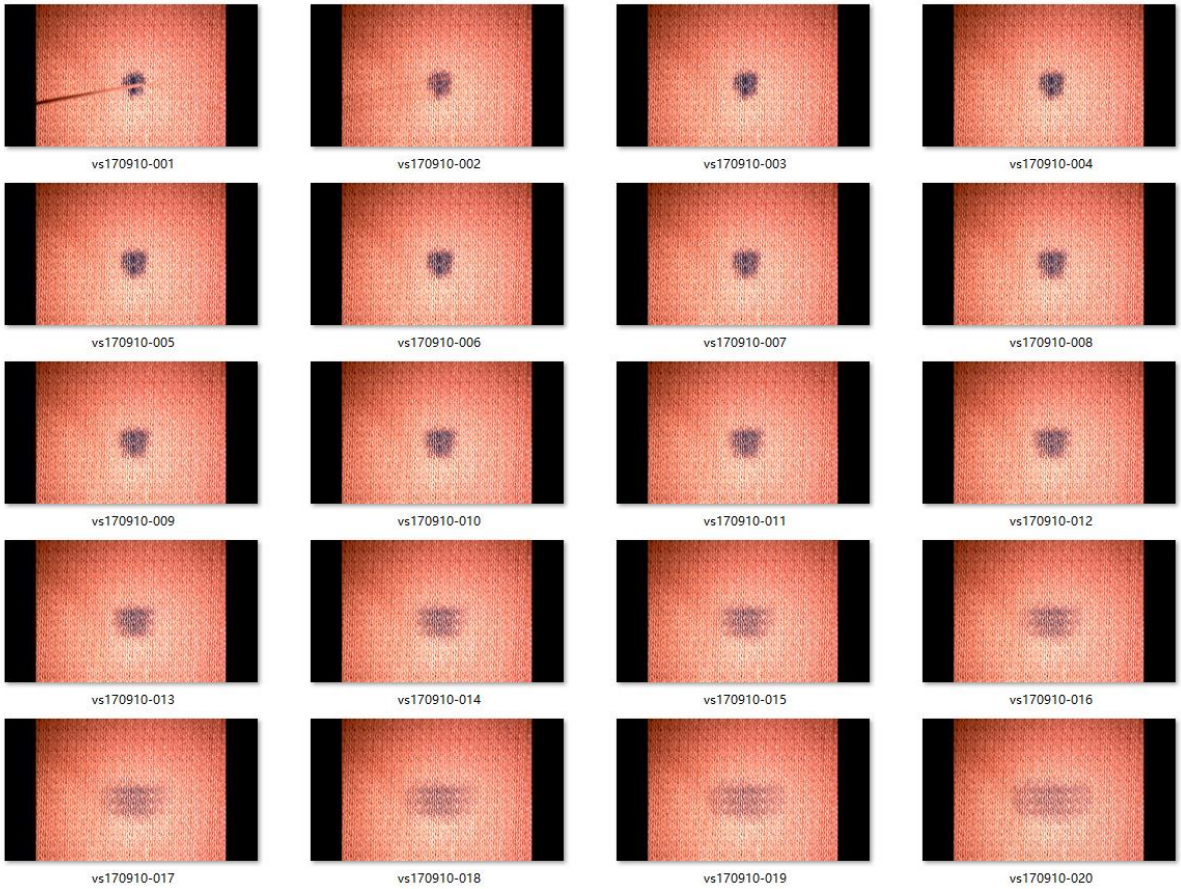
vs170910-001
vs170910-002
vs170910-003
vs170910-004
vs170910-005
vs170910-006
vs170910-007
vs170910-008
vs170910-009
vs170910-010
vs170910-011
vs170910-012
vs170910-013
vs170910-014
vs170910-015
vs170910-016
vs170910-017
vs170910-018
vs170910-019
vs170910-020